J. Fluid Mech. (2012), *vol.* 709, *pp.* 313–340.
doi:10.1017/jfm.2012.336

Transmission of acoustic-gravity waves through gas–liquid interfaces

Oleg A. Godin[1,2]† **and Iosif M. Fuks**[2,3]

[1] Cooperative Institute for Research in Environmental Sciences, University of Colorado at Boulder, Boulder, CO 80309-0216, USA

[2] NOAA/Earth System Research Laboratory, Physical Sciences Division, Boulder, CO 80305-3328, USA

[3] Zel Technologies LLC, Boulder, CO 80305-3328, USA

(Received 6 April 2012; revised 25 June 2012; accepted 27 June 2012; first published online 10 August 2012)

It was demonstrated recently that gas–liquid interfaces, which are usually almost perfect reflectors of acoustic waves, become anomalously transparent, and the power flux in the wave transmitted into the gas increases dramatically, when a compact sound source in the liquid approaches the interface within a fraction of the wavelength (Godin, *Phys. Rev. Lett.*, vol. 97, 2006*b*, 164301). Powerful underwater explosions and certain natural sources, such as underwater landslides, generate very low-frequency waves in water and air, for which fluid buoyancy and compressibility simultaneously serve as restoring forces. In this paper, analysis of sound transmission through gas–liquid interfaces is extended to acoustic-gravity waves (AGWs) and applied to the air–water interface. It is found that, as for sound, the interface becomes anomalously transparent for sufficiently shallow compact sources of AGWs. Depending on the source type, the increase of a wave power flux into gas due to diffraction effects can reach several orders of magnitude. The physical mechanisms responsible for the anomalous transparency are discussed. Excitation of an interface wave by a point source in the liquid is shown to be an important channel of AGW transmission into the gas, which has no counterpart in the case of sound.

Key words: air/sea interactions, surface gravity waves, wave scattering

1. Introduction

The interaction between wave processes in the ocean and atmosphere is encountered in problems as diverse and important as the quantification of the climate implications of energy, momentum and gas fluxes at air–sea interactions (Kemball-Cook & Wang 2001; Hristov, Miller & Friehe 2003; Sullivan & McWilliams 2010), early tsunami detection and warning with satellite-borne instruments (Godin 2004; Artru *et al.* 2005; Godin *et al.* 2009; Rolland *et al.* 2010), and infrasonic detection of underwater explosions for the purposes of the Comprehensive Nuclear Test Ban Treaty (Evers & Haak 2001; Drob *et al.* 2010).

In atmospheric and underwater acoustics and in marine seismology, air–water interfaces are usually approximated by a perfectly reflecting boundary. It has been

† Email address for correspondence: oleg.godin@noaa.gov

found recently (Godin 2006*b*, 2007, 2008*a*,*b*) that low-frequency acoustic fields in the ocean and atmosphere are much more closely connected than was previously believed possible.

Under normal conditions, when a monopole, point underwater sound source with a fixed magnitude of volume velocity oscillations approaches the air–water interface, the acoustic power flux into the air increases by a factor of $\sim$40 compared to the power flux from the same source at depths of one wavelength or more. The transparency of the interface, which is defined as the ratio of the power transmitted to the interface to the total radiated power, increases by a factor of 3400 and closely approaches unity (Godin 2006*b*, 2007, 2008*b*). Thus, most of the acoustic energy emitted by a shallow, compact, underwater source is radiated into the air. More generally, the anomalous increase in the transparency can occur when the sound source is located in a denser fluid with a higher sound speed, such as a liquid, at a fraction of the wavelength from a flat or rough interface with a lighter fluid with a smaller sound speed, such as a gas. Mathematically, a fluid–fluid interface is anomalously transparent for shallow sources provided it is characterized by two dimensionless small parameters: the ratio of mass densities, and the ratio of sound speeds squared (Godin 2006*b*, 2007, 2008*b*). Physically, the anomalous transparency is due, first, to the contribution of evanescent waves in the liquid into the power flux from the source to the interface, and, second, to the destructive interference between direct and interface-reflected waves in the liquid (Godin 2006*b*, 2007; McDonald & Calvo 2007).

In acoustics, the lower the frequency, the more pronounced are the diffraction effects responsible for the anomalous transparency (Godin 2008*b*). However, at sufficiently low frequencies (below $\sim$1 Hz for air–water interfaces), buoyancy effects may become significant and need to be taken into account. The question arises whether the anomalous transparency of gas–liquid interfaces is a purely acoustical phenomenon or does it also take place for acoustic-gravity waves (AGWs), for which fluid buoyancy and compressibility simultaneously serve as restoring forces (Lamb 1932; Press & Harkrider 1962; Tolstoy 1973; Lighthill 1978). Here, we consider in a simple, idealized setting the problem of transmission into a gas of AGWs generated by a compact source in a liquid. We will show that, as for sound, gas–liquid interfaces become anomalously transparent, when the source is sufficiently close to the interface, but the physical mechanisms responsible for the anomalous transparency are distinct for sound and AGWs.

For sound, the simplest transmission problem involves a plane interface of two homogeneous fluid half-spaces (Brekhovskikh & Godin 1998, 1999). Mass density necessarily increases downwards in stably stratified compressible fluids in a gravity field. A basic self-consistent environmental model suitable for AGW propagation analysis is a fluid with a constant sound speed and an exponential stratification of density. Such a model allows for plane-wave solutions and has been studied extensively in the past (Lamb 1932; Eckart 1960; Pierce 1963; Tolstoy 1963; Gossard & Hooke 1975; Adam 1977; Watada 2009). The simplest environmental model for the AGW transmission problem consists of two fluid half-spaces, each with its own constant sound speed and exponential density profile, separated by a horizontal plane. AGWs in such an environment have been considered by a number of authors. Tolstoy (1973) discussed reflection and transmission of plane waves at the interface. The properties of surface waves supported by the interface have also been considered (Lamb 1911, 1932; Tolstoy 1963; Thome 1968; Gossard & Hooke 1975; Savina 1997; Gasilova & Petukhov 1999). Petukhov and co-workers developed a semi-analytic description of excitation of the surface waves by a point source (Petukhov 1992;

Gasilova, Gordeeva & Petukhov 1992, 1993; Gasilova & Petukhov 1993, 1999). Unlike earlier work on the subject, here we account for all waves generated by a compact source, investigate power fluxes in the body and surface AGWs, identify previously unknown, resonance-like dramatic increases in the interface transparency at certain frequencies, and determine the physical causes of their origin.

Several particular types of monochromatic AGWs feature prominently in our analysis. Plane waves with a real-valued wave vector will be referred to as 'homogeneous' or 'propagating' plane waves. Waves with a complex-valued wave vector are known as 'inhomogeneous' plane waves since their amplitude is not homogeneous along their wave front (Brekhovskikh & Godin 1998). In particular, when considered in a bounded region and their amplitude decreases exponentially away from the boundary, inhomogeneous waves are also called 'evanescent' plane waves. AGWs that are supported by an unbounded fluid are referred to as 'body' waves. On the other hand, AGWs that propagate along a fluid–fluid interface and rapidly attenuate with increasing distance from the interface will be interchangeably called 'surface' or 'interface' waves. In the case of a gas–liquid interface, we will encounter 'modified Lamb waves', which are an extension of surface waves propagating in a gas half-space along a plane rigid boundary (Lamb 1932; Gossard & Hooke 1975), and 'modified surface gravity waves', which are an extension of surface waves in a liquid half-space with a free surface (Lamb 1932; Brekhovskikh & Goncharov 1994).

The paper is organized as follows. Governing equations and boundary conditions for AGWs are formulated in § 2. Reflection and transmission coefficients for plane AGWs at a plane fluid–fluid interface are derived in § 3. Dispersion relations of surface waves supported by a gas–liquid interface, their cutoff frequencies and excitation by a point source are studied asymptotically in § 4 using the ratio of gas and fluid densities as a small parameter of the theory. Energy radiated by a point source in liquid into gas and liquid half-spaces in body and surface waves is studied in § 5. The physical mechanisms responsible for the normal and anomalous transparency of gas–liquid interfaces for AGWs are discussed and compared to the acoustic case in § 6. Section 7 summarizes our findings.

2. Point source in a layered fluid

Consider mechanical waves in a stationary, inhomogeneous compressible fluid in a uniform gravity field. Linear monochromatic (continuous wave, CW) wave fields are governed by the equations (see e.g. Tolstoy 1963; Godin 1997; Brekhovskikh & Godin 1999)

$$\nabla p - \omega^2 \rho \boldsymbol{w} + (\boldsymbol{w} \cdot \nabla)\nabla p_0 - (p + \boldsymbol{w} \cdot \nabla p_0)\nabla p_0/\rho c^2 = \boldsymbol{F}, \tag{2.1}$$

$$\nabla \cdot \boldsymbol{w} + (p + \boldsymbol{w} \cdot \nabla p_0)/\rho c^2 = iA/\omega, \tag{2.2}$$

where p_0, c and ρ are the pressure, sound speed and mass density unperturbed by the wave; p and $\boldsymbol{w}$ are pressure perturbations and fluid parcel displacements due to the wave; and ω is wave frequency. Equations (2.1) and (2.2) are obtained from linearized Euler, continuity and state equations by eliminating unknown wave-induced mass density perturbations. The gradient of the background pressure is given by $\nabla p_0 = \rho \boldsymbol{g}$, where $\boldsymbol{g}$ is the acceleration due to gravity. Wave energy dissipation through irreversible thermodynamic processes is neglected. The wave field is generated by sources with volume densities $\boldsymbol{F}$ of force and A of volume velocity. A time dependence $\exp(-\mathrm{i}\omega t)$ of the wave field is assumed and suppressed.

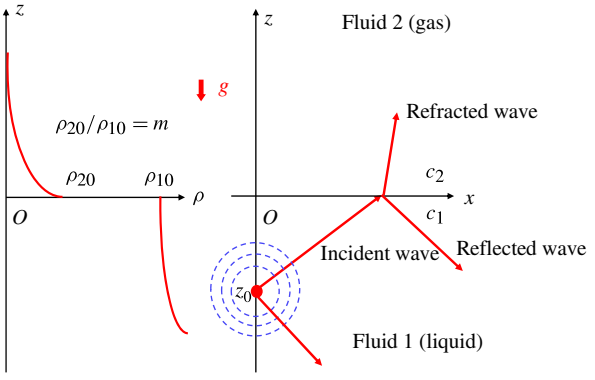

FIGURE 1. (Colour online) Geometry of the problem.

At a fluid–fluid interface S (i.e. a surface where sound speed and/or density are discontinuous), the boundary conditions for linear waves are (see e.g. Godin 1997; Brekhovskikh & Godin 1999)

$$[\boldsymbol{w}\cdot\boldsymbol{n}]_S = 0, \quad [p + \boldsymbol{w}\cdot\nabla p_0]_S = 0, \tag{2.3}$$

where $\boldsymbol{n}$ is a unit normal to S and $[f]_S$ denotes the jump of a function f at a point on the surface S. The first equation in (2.3) expresses the kinematic boundary condition of the continuity of the normal component of the fluid velocity on the interface, while the second equation expresses the dynamic boundary condition of the continuity of the full pressure, $p_0 + p$, on the perturbed interface. The quantity $p + \boldsymbol{w}\cdot\nabla p_0$ has a meaning of pressure perturbation in a moving fluid parcel (Lagrangian perturbation), while p is the pressure perturbation at a given point (Eulerian perturbation). Alternatively, $p + \boldsymbol{w}\cdot\nabla p_0$ can be viewed as a linear perturbation of the full pressure at a point on the interface deformed by the wave.

We now introduce Cartesian coordinates $\boldsymbol{R} = (x, y, z)$ with horizontal coordinates x, y and vertical coordinate z directed upwards, so that $\boldsymbol{g} = -g\nabla z$, $g = \text{const.} > 0$ (figure 1). Let a point source be located at $\boldsymbol{R}_0 = (0, 0, z_0)$,

$$A = A_0\delta(x)\delta(y)\delta(z - z_0), \quad \boldsymbol{F} = \boldsymbol{F}_0\delta(x)\delta(y)\delta(z - z_0), \tag{2.4}$$

and let the unperturbed sound speed and density be independent of the horizontal coordinates. In such a layered medium, (2.1) and (2.2) can be solved in terms of quasi-plane waves, i.e. waves with harmonic dependence $\exp(\mathrm{i}\boldsymbol{q}\cdot\boldsymbol{R})$, where $\boldsymbol{q} = (q_x, q_y, 0) = \text{const.}$ on horizontal coordinates (see e.g. Brekhovskikh & Godin 1998, 1999). For free quasi-plane waves, equations (2.1) and (2.2) give

$$\frac{\partial p}{\partial z} + \frac{g}{c^2}p = \rho(\omega^2 - N^2)w_z, \quad \frac{\partial w_z}{\partial z} - \frac{g}{c^2}w_z = \left(\frac{q^2}{\omega^2\rho} - \frac{1}{\rho c^2}\right)p, \tag{2.5}$$

$$w_x = \frac{\mathrm{i}q_x}{\omega^2\rho}p, \quad w_y = \frac{\mathrm{i}q_y}{\omega^2\rho}p, \quad N^2 = -\frac{g}{\rho}\frac{\mathrm{d}\rho}{\mathrm{d}z} - \frac{g^2}{c^2}. \tag{2.6}$$

Here, q is the magnitude of vector $\boldsymbol{q}$, and N has the meaning of the buoyancy frequency. Note that the vertical structure of the wave field is independent of the direction of the horizontal vector $\boldsymbol{q}$. By eliminating w_z, (2.5) can be readily reduced to a second-order differential equation for p.

By applying the Fourier transform in x and y (or, alternatively, the Fourier–Bessel transform in the horizontal plane) to (2.1) and (2.2) and taking into account (2.4), for the field due to a point source, we find

$$p(\boldsymbol{R}, z_0) = \left\{ \left(1 - \frac{N^2}{\omega^2}\right) \left[\mathrm{i}\omega\rho A_0 + F_{0x}\frac{\partial}{\partial x} + F_{0y}\frac{\partial}{\partial y} \right] - F_{0z}\left[\frac{g}{c^2} + \left(\frac{\partial}{\partial z} \ln\rho \left(1 - \frac{N^2}{\omega^2}\right)\right) + \frac{\partial}{\partial z_0} \right] \right\}_{z=z_0} P(\boldsymbol{R}, z_0), \tag{2.7}$$

$$P(\boldsymbol{R}, z_0) = \int_{-\infty}^{+\infty} \int \frac{p_1(q, z_<)p_2(q, z_>)}{4\pi^2 W_r(q, z_0)} \mathrm{e}^{\mathrm{i}\boldsymbol{q}\cdot\boldsymbol{R}}\, \mathrm{d}q_1\, \mathrm{d}q_2 = \int_{-\infty}^{+\infty} \frac{p_1(q, z_<)p_2(q, z_>)}{4\pi W_r(q, z_0)} H_0^{(1)}(qr) q\, \mathrm{d}q, \tag{2.8}$$

where $W_r(q, z) = p_1(q, z)\partial p_2(q, z)/\partial z - p_2(q, z)\partial p_1(q, z)/\partial z$, $z_< = \min(z, z_0)$, $z_> = \max(z, z_0)$, $r = (x^2 + y^2)^{1/2}$ and $H_0^{(1)}(\cdot)$ is the Hankel function. Here p_1 and p_2 are the solutions to (2.5) that satisfy conditions at $z \to -\infty$ (or at the lower boundary in the case of a bounded medium) and at $z \to +\infty$ (or at the upper boundary), respectively. It is assumed that c, ρ and $\mathrm{d}\rho/\mathrm{d}z$ are continuous at $z = z_0$. Note that q is non-negative in the first integral in (2.8). The second integral is taken over all real q and, with $p_{1,2}$ being analytic functions of q, can be viewed as a contour integral in the complex q plane. When $g \to 0$, (2.7) and (2.8) reduce to known results for acoustic fields (Godin 2006*a*).

Application of the Fourier transform reduces (2.1) and (2.2) to a homogeneous ordinary differential equation for $p(q, z)$ at $z > z_0$ and $z < z_0$, with the source terms in (2.1) and (2.2) giving matching conditions at $z = z_0$. To ensure sufficiently rapid decrease of the wave field with r and justify application of the Fourier transform, one considers monochromatic waves as a limiting case of a wave field growing with time and assigns an infinitesimal, positive imaginary part to the frequency ω. The derivation of (2.7) and (2.8) for AGWs is analogous to the derivation in the acoustic case ($g = 0$), which is discussed in detail in § 4.3.2 of Brekhovskikh & Godin (1999) for a source of volume velocity ($\boldsymbol{F} = 0$), and will not be reproduced here. An equation similar to (2.7) and (2.8) has been derived by Pierce (1965) for AGWs generated by a point source of volume velocity.

3. Reflection and transmission of plane waves

Let horizontal interface $z = 0$ separate fluid half-spaces with constant sound speeds c_1 and c_2 and mass densities $\rho_1(z)$ and $\rho_2(z)$ at $z < 0$ and $z > 0$, respectively (figure 1). The densities decrease exponentially with height:

$$\rho_j(z) = \rho_{j0}\exp(-2\mu_j z), \quad \mu_j \geqslant 0, \quad j = 1, 2. \tag{3.1}$$

In particular, for an isothermal perfect gas, $\mu_j = \gamma_j g/2c_j^2$, where γ is the ratio of the specific heats at constant pressure and constant volume (Eckart 1960). Buoyancy frequencies N_j (2.6) are constant in both half-spaces, and (2.5) have plane-wave solutions (Eckart 1960; Pierce 1963; Tolstoy 1963, 1973)

$$p^{(j)} = \exp[\mathrm{i}\boldsymbol{q}\cdot\boldsymbol{R} \pm \mathrm{i}s_j(q)z - \mu_j z], \quad w_z^{(j)} = B_\pm^{(j)}\exp[\mathrm{i}\boldsymbol{q}\cdot\boldsymbol{R} \pm \mathrm{i}s_j(q)z + \mu_j z], \tag{3.2}$$

where

$$B_{\pm}^{(j)} = \frac{gc_j^{-2} - \mu_j \pm \mathrm{i}s_j}{\rho_{j0}(\omega^2 - N_j^2)}, \quad N_j^2 = 2g\mu_j - \frac{g^2}{c_j^2}, \tag{3.3}$$

$$s_j(q) = \sqrt{\omega^2 c_j^{-2} - \mu_j^2 - q^2(1 - N_j^2/\omega^2)}, \quad \operatorname{Im} s_j \geqslant 0, \tag{3.4}$$

and s_j is either non-negative or purely imaginary. Note that, in stably stratified media, $\rho_{10} \geqslant \rho_{20}, N_j^2 \geqslant 0$ (Tolstoy 1973) and, hence, $\mu_j \geqslant g/2c_j^2$.

Equation (3.4) is a form of the well-known dispersion relation of acoustic-gravity waves (see e.g. Tolstoy 1963, 1973; Gossard & Hooke 1975; Lighthill 1978). Taken with the appropriate sign, s_j has the meaning of the vertical component of the wave vector of plane waves (3.2). Propagating plane waves, i.e. waves with real q and s_j, exist at $\omega < N_j$ (the buoyancy branch of AGWs) and $\omega > \mu_j c_j$ (the acoustic branch of AGWs). It follows from (2.6) and (3.1) that $\mu_j^2 c_j^2 - N_j^2 = (\mu_j c_j - g/c_j)^2$ and, hence, $\mu_j c_j \geqslant N_j$. There are no propagating plane waves at $N_j < \omega < \mu_j c_j$ (which certainly does not mean that point AGW sources generate no perturbations at such frequencies). Below, we assume for definiteness that the stratification is stable and, unless stipulated to the contrary, that $\omega \geqslant \max(\mu_1 c_1, \mu_2 c_2)$.

The time-averaged energy density E (away from the interfaces) and power flux $\boldsymbol{I}$ in monochromatic AGWs (Tolstoy 1973; Brekhovskikh & Godin 1999) are

$$E = \frac{\rho}{4}\left(\omega^2 \boldsymbol{w}\cdot\boldsymbol{w}^* + N^2 w_z w_z^* + \frac{pp^*}{\rho^2 c^2}\right), \quad \boldsymbol{I} = \frac{\omega}{2}\operatorname{Im}(p^*\boldsymbol{w}), \tag{3.5}$$

where the asterisk denotes complex conjugation. When applied to plane waves (3.2), these equations show that the choice of the upper (lower) sign in (3.2) gives waves that carry energy upwards (downwards) when $s_j > 0$; when $\operatorname{Re} s_j = 0$, the power flux is horizontal and only the choice of upper (lower) sign ensures finiteness of the energy density at $z \to +\infty$ (respectively, $z \to -\infty$).

Let a plane wave $p = \exp[\mathrm{i}\boldsymbol{q}\cdot\boldsymbol{R} + \mathrm{i}s_1(q)z - \mu_1 z]$ be incident on the interface $z = 0$ from below. Then pressure perturbations in the lower and upper half-spaces are

$$p = \exp[\mathrm{i}\boldsymbol{q}\cdot\boldsymbol{R} + \mathrm{i}s_1(q)z - \mu_1 z] + V(q)\exp[\mathrm{i}\boldsymbol{q}\cdot\boldsymbol{R} - \mathrm{i}s_1(q)z - \mu_1 z], \quad z < 0, \tag{3.6a}$$

$$p = W(q)\exp[\mathrm{i}\boldsymbol{q}\cdot\boldsymbol{R} + \mathrm{i}s_2(q)z - \mu_2 z], \quad z > 0, \tag{3.6b}$$

where V and W have the meaning of reflection and transmission coefficients (with respect to pressure). Boundary conditions (2.3) on the interface $z = 0$ give two linear algebraic equations for V and W, from which we find

$$V = -D_+/D_-, \quad W = 2m(\omega^2 - N_2^2)s_1 D_-, \tag{3.7}$$

$$D_{\pm} = \left(\frac{\mathrm{i}}{g}N_2^2 - \mathrm{i}\mu_2 + s_2\right)(\omega^2 - g\mu_1 \mp \mathrm{i}gs_1) - m\left(\frac{\mathrm{i}}{g}N_1^2 - \mathrm{i}\mu_1 \pm s_1\right)(\omega^2 - g\mu_2 - \mathrm{i}gs_2), \tag{3.8}$$

where $m = \rho_{20}/\rho_{10}$ is the ratio of fluid densities at the interface. Similar equations were derived by Tolstoy (1973). When a plane wave is incident on the interface from the upper half-space, reflection and transmission coefficients can be obtained from (3.7) and (3.8) by interchanging indices 1 and 2 and replacing g with $-g$.

When the incident wave is a propagating one ($\operatorname{Im} s_1 = 0$) and the refracted wave is evanescent ($\operatorname{Re} s_2 = 0$), $D_+ = -D_-^*$ and $|V| = 1$, as expected. At $g \to 0$, from (3.7) and (3.8) one recovers the well-known Fresnel reflection and transmission

coefficients, $V=(ms_1-s_2)/(ms_1+s_2)$ and $W=2ms_1/(ms_1+s_2)$ (see e.g. Brekhovskikh & Godin 1998) for acoustic waves. In the limits $m\to 0$ and $m\to\infty$, equations (3.7) and (3.8) give

$$V=-(\omega^2-g\mu_1-\mathrm{i}gs_1)/(\omega^2-g\mu_1+\mathrm{i}gs_1), \tag{3.9}$$

$$V=(s_1-\mathrm{i}\mu_1+\mathrm{i}N_1^2/g)/(s_1+\mathrm{i}\mu_1-\mathrm{i}N_1^2/g). \tag{3.10}$$

Equations (3.9) and (3.10) do not contain parameters of the upper half-space and have the meaning of reflection coefficients from the free and rigid boundaries, respectively. At the free and rigid boundaries, $|V|=1$ for homogeneous plane waves. At the gas–liquid interface, m is small, the reflection coefficient V in (3.7) is close to its value (3.9) for the free surface and $|V|=1+O(m)$ as long as both the incident and transmitted waves are propagating ones (figure 2*a*). At grazing incidence, when $s_1=0$, $V=-1$ at a gas–liquid interface. However, additional singularities of the reflection coefficient appear when both waves are evanescent ($\mathrm{Re}\,s_1=\mathrm{Re}\,s_2=0$) (figure 2*b*,*c*). In § 4 we show that these singularities are a manifestation of the interface waves supported by the gas–liquid interface but not by the free surface. The numerical values in figure 2 and all subsequent figures refer to a water–air interface with $m=1.3\times10^{-3}$, $c_1=1500$ m s^{-1}, $c_2=330$ m s^{-1}, $\mu_1=3.56\times10^{-6}$ m^{-1}, $\mu_2=6.30\times10^{-5}$ m^{-1} and $g=9.8$ m s^{-2}. The dimensionless wave frequency is defined as $f=\omega/\omega_0$, where the reference frequency $\omega_0=g/c_2$ corresponds to 4.73×10^{-3} Hz (i.e. to a wave period of 211 s) for the water–air interface. The physical significance of the frequency ω_0 is discussed in § 4.4.

Equations (3.3) and (3.5) show that, for plane waves with $s_j>0$, the directions of the vertical component of the power flux are opposite at $\omega>N_j$ and $\omega<N_j$. For incident and reflected waves, this translates into opposite choices of the sign in front of s_j in (3.2) at high and low frequencies. Inspection shows that (3.6)–(3.8), which have been derived above assuming $\omega\geqslant\max(\mu_1c_1,\mu_2c_2)$, remain valid at all frequencies if $\mathrm{i}s_j$ is replaced with the complex conjugate, $(\mathrm{i}s_j)^*$, when $\omega<N_j$. This has been taken into account in figure 2. Note that no changes occur when $\mathrm{Re}\,s_j=0$.

4. Interface waves

4.1. *Dispersion equation of surface AGWs at a fluid–fluid interface*

Let a point source be located in the lower half-space $z<0$. According to (3.2) and (3.6), the solutions $p_{1,2}$ in (2.8) can be chosen as

$$p_1=\mathrm{e}^{-\mathrm{i}s_1z-\mu_1z},\quad z<0; \tag{4.1}$$

$$p_2=\mathrm{e}^{\mathrm{i}s_1z-\mu_1z}+V\mathrm{e}^{-\mathrm{i}s_1z-\mu_1z},\quad z<0;\quad p_2=W\mathrm{e}^{\mathrm{i}s_2z-\mu_2z},\quad z>0. \tag{4.2}$$

Here the reflection V and transmission W coefficients are given by (3.7). From (2.7), (2.8), (4.1) and (4.2) we obtain the field due to a point source as an integral over plane or cylindrical waves:

$$\begin{aligned}P(\boldsymbol{R},z_0)&=\frac{\mathrm{e}^{\mu_1(z_0-z)}}{8\mathrm{i}\pi^2}\int_{-\infty}^{+\infty}\int_{-\infty}^{+\infty}\frac{\mathrm{d}q_1\,\mathrm{d}q_2}{s_1}[\mathrm{e}^{\mathrm{i}s_1|z-z_0|}+V\mathrm{e}^{-\mathrm{i}s_1(z+z_0)}]\mathrm{e}^{\mathrm{i}\boldsymbol{q}\cdot\boldsymbol{R}}\\&=\frac{\mathrm{e}^{\mu_1(z_0-z)}}{8\mathrm{i}\pi}\int_{-\infty}^{+\infty}\frac{q\,\mathrm{d}q}{s_1}[\mathrm{e}^{\mathrm{i}s_1|z-z_0|}+V\mathrm{e}^{-\mathrm{i}s_1(z+z_0)}]H_0^{(1)}(qr),\quad z<0;\end{aligned} \tag{4.3}$$

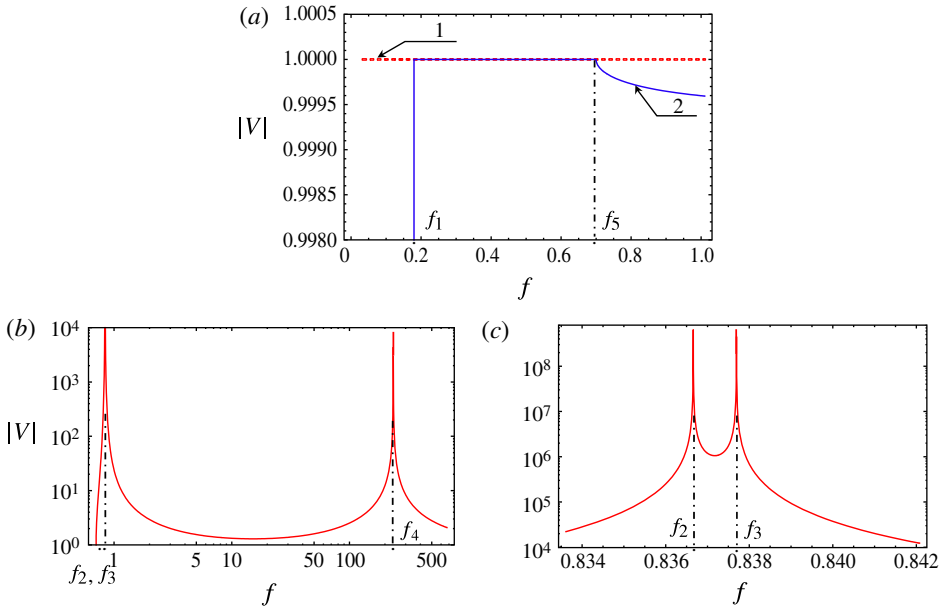

FIGURE 2. (Colour online) Reflection of plane acoustic-gravity waves from a gas–liquid interface. Absolute value of the reflection coefficient (3.7) is shown as a function of dimensionless frequency $f = \omega/\omega_0$ for waves incident from water on a water–air interface at (*a*) $s_1 = 0$ (incident and reflected waves propagate along the interface; line 1) and $q = 0$ (normal incidence; line 2); and (*b*) $s_2 = 0$ (refracted wave propagates along the interface). (*c*) A detailed view of a segment of (*b*). Frequencies $f_j = \omega_c^{(j)}/\omega_0$, $j = 1, 2, 3, 4$, correspond to the cutoff frequencies (4.11), (4.16) and (4.21) of interface waves; $f_5 = \mu_2 c_2/\omega_0$. The reflection coefficient has singularities (poles) at $f = f_2, f_3, f_4$.

$$P(\boldsymbol{R}, z_0) = \frac{\mathrm{e}^{\mu_1 z_0 - \mu_2 z}}{8\mathrm{i}\pi^2} \int_{-\infty}^{+\infty} \int_{-\infty}^{+\infty} \frac{\mathrm{d}q_1\, \mathrm{d}q_2}{s_1} W \mathrm{e}^{\mathrm{i}\boldsymbol{q}\cdot\boldsymbol{R} - \mathrm{i}s_1 z_0 + \mathrm{i}s_2 z}$$
$$= \frac{\mathrm{e}^{\mu_1 z_0 - \mu_2 z}}{8\mathrm{i}\pi} \int_{-\infty}^{+\infty} \frac{q\, \mathrm{d}q}{s_1} W \mathrm{e}^{\mathrm{i}s_2 z - \mathrm{i}s_1 z_0} H_0^{(1)}(qr), \quad z > 0. \tag{4.4}$$

The integrands of the right-most sides of (4.3) and (4.4) are analytic functions of q. The contributions of poles $q = q_p$ of the integrands to P have the meaning of interface waves generated by the source and usually provide the dominant component of the field at sufficiently large r (Brekhovskikh & Godin 1999). When $\mathrm{Im}\, q_p = 0$, one obtains proper surface waves, which propagate along the interface with phase speed ω/q_p.

According to (3.7) and (3.8), the locations of all poles in the complex q plane are given by solutions of the algebraic equation $D_-(q) = 0$, or

$$\left(\frac{\mathrm{i}}{g}N_2^2 - \mathrm{i}\mu_2 + s_2\right)(\omega^2 - g\mu_1 + \mathrm{i}g s_1) = m\left(\frac{\mathrm{i}}{g}N_1^2 - \mathrm{i}\mu_1 - s_1\right)(\omega^2 - g\mu_2 - \mathrm{i}g s_2). \tag{4.5}$$

Note that the poles of the reflection and transmission coefficients (3.7) coincide; i.e. the same interface waves are observed in the upper and lower half-spaces. Analysis

of the integral representation of a field due to a point source located in the upper half-space also leads to the dispersion equation (4.5) of interface waves. Moreover, the dispersion equation (but not the contributions of interface waves to the field due to a point source) can also be found by considering plane-wave solutions (3.2) at $z > 0$ and $z < 0$ with energy density decaying exponentially away from the interface, and imposing the boundary conditions (2.3) on these solutions.

It follows from the energy conservation law that $\operatorname{Im} s_j(q_p) > 0$, $j = 1, 2$, for interface waves (Brekhovskikh & Godin 1998). These inequalities ensure that the energy and power flux densities (3.5) remain finite in the interface waves at all z. Often interface waves exist only in a certain frequency range or ranges bounded from above and/or from below by a cutoff frequency ω_c. According to (3.4), when $q_p(\omega)$ is real and varies continuously with ω, $s_j(q_p)$ ceases to have a positive imaginary part when s_j becomes equal to zero. Hence, for proper surface waves, $s_1 s_2 = 0$ at each cutoff frequency. It follows from (3.4) and (4.5) that ω_c^2 satisfies the following fourth-order algebraic equation:

$$\begin{aligned}(-1)^j(\omega_c^2 - N_j^2)\left[\omega_c^2\left(\mu_2 - \frac{N_2^2}{g} - m\mu_1 + m\frac{N_1^2}{g}\right)\right.\\ \left. - \mu_1(g\mu_2 - N_2^2) + m\mu_2(g\mu_1 - N_1^2)\right]^2\\ = \left[(\omega_c^2 - N_2^2)\left(\mu_1^2 - \frac{\omega_c^2}{c_1^2}\right) - (\omega_c^2 - N_1^2)\left(\mu_2^2 - \frac{\omega_c^2}{c_2^2}\right)\right]\\ \times\left[m^{j-1}(\omega_c^2 - g\mu_j) + m^{2-j}(g\mu_j - N_j^2)\right]^2, \end{aligned} \tag{4.6}$$

with either $j = 1$ or $j = 2$. For (4.6) and the results presented below in § 4 to be valid, there is no need to restrict the frequency range by the assumuption $\omega \geqslant \max(\mu_1 c_1, \mu_2 c_2)$.

No analytic solution of the dispersion equation (4.5) is available in the general case. However, when $c_1 = c_2$ and $\mu_1 = \mu_2$, we have $N_1 = N_2$ and $s_1 = s_2$. Then (4.5) becomes a quadratic equation and gives

$$s_1 = \mathrm{i}\frac{(\omega^2 - N_1^2)(1+m)}{2g(1-m)}(1 \pm \zeta), \quad q^2 = \frac{\omega^2\mu_1}{g} + \frac{\omega^2(\omega^2 - N_1^2)\,(1+m)^2}{2g^2\,(1-m)^2}(1 \pm \zeta), \tag{4.7a}$$

$$\zeta = \sqrt{1 + 4\left(\frac{1-m}{1+m}\right)^2 \frac{(\omega^2 - g\mu_1)(N_1^2 - g\mu_1)}{(\omega^2 - N_1^2)^2}}. \tag{4.7b}$$

When $m \to 0$, the right-hand side of (4.5) vanishes, and the dispersion equation has two solutions:

$$s_1 = \mathrm{i}(\omega^2/g - \mu_1), \quad q = \omega^2/g, \tag{4.8}$$

$$s_2 = \mathrm{i}(gc_2^{-2} - \mu_2), \quad q = \omega/c_2. \tag{4.9}$$

The first solution, (4.8), is independent of the parameters of the upper half-space, describes a surface wave at $z < 0$ provided $\omega^2 > g\mu_1$, and represents a familiar 'surface gravity wave in deep water', i.e. a surface wave in a fluid half-space with a free upper boundary (Lamb 1932; Brekhovskikh & Goncharov 1994). The second solution, (4.9), is independent of the parameters of the lower half-space, describes a surface wave at $z > 0$ provided $\mu_2 < gc_2^{-2}$, and represents a familiar Lamb wave (Lamb 1932; Gossard

& Hooke 1975), i.e. a surface AGW in a fluid half-space with a constant sound speed and a rigid lower boundary. When $\omega^2 \leqslant g\mu_1$ or $\mu_2 \geqslant gc_2^{-2}$, the corresponding surface wave does not exist. Below, we will assume that $\mu_1 \leqslant \mu_2$, $\omega^2 > g\mu_1$ and

$$\mu_j \leqslant gc_j^{-2} \leqslant 2\mu_j \tag{4.10}$$

for definiteness, and investigate how the surface waves (4.8) and (4.9) are modified when m is small but finite. Note that strict inequalities always hold in (4.10) for perfect gases (Lamb 1932; Gossard & Hooke 1975), and $\mu_1 \ll \mu_2$ in the case of the ocean–atmosphere interface.

4.2. *Modified surface gravity wave at a gas–liquid interface*

When q is given by (4.8), $s_2 = \mathrm{i}|\omega^2/g - \mu_2|$ according to (3.4), and the right-hand side of the dispersion equation (4.5) equals zero for all m values provided

$$\omega_c^{(1)} < \omega < \omega_c^{(2)}, \quad \omega_c^{(j)} = \sqrt{g\mu_j}, \quad j = 1, 2. \tag{4.11}$$

In the frequency range (4.11), an interface AGW with the dispersion equation $\omega^2 = gq$ propagates along the fluid–fluid interface. Frequencies $\omega_c^{(j)}$ in (4.11) satisfy (4.6), give $s_j = 0$ and are cutoff frequencies of the interface wave. The phase and group speeds of the interface wave are unaffected by the presence of the upper half-space and independent of the sound speeds in the two fluids and of the density jump, if any, at the interface. In this interface wave, according to (2.6), (3.2), (3.5) and (4.8), the wave energy density decreases exponentially with distance from the interface, the vertical displacement has exponential dependence $w_z(z) = w_z(0)\exp(\omega^2 z/g)$ throughout the fluid, the horizontal displacement is $w_{x,y}(z) = \mathrm{i}q^{-1}q_{x,y}w_z(z)$, and the Lagrangian pressure perturbation $\tilde{p} = p - \rho g w_z$ is identically zero. The independence of the dispersion equation from the sound speed is easy to understand since the motion in the interface wave is incompressible: $\boldsymbol{\nabla} \cdot \boldsymbol{w} = 0$. Lamb (1911, pp. 568–571) considered surface AGWs propagating along a horizontal interface of two isothermal gases of different temperature. He assumed, erroneously, that the particle displacement necessarily decreases with height at $z > 0$ in surface waves and, therefore, was not able to find the surface wave with the dispersion equation (4.8).

A wave with $\tilde{p} = 0$, $w_z(z) = w_z(0)\exp(\omega^2 z/g)$ and $q = \omega^2/g$ satisfies the equations of motion (2.5) and the boundary conditions at $z = 0$ at arbitrary frequencies, but carries finite power flux only under condition (4.11). This wave is a particular case of the incompressible wave motion of compressible fluids, which can exist in bounded and unbounded domains with arbitrary stratification (Godin 2012*a*).

To solve the general dispersion equation (4.5) beyond the frequency interval (4.11), we search for a solution in terms of a development in powers of m that reduces to (4.8) at $m = 0$, and obtain

$$q = \frac{\omega^2}{g}[1 + \alpha_1 m + 2\alpha_2 m^2 + O(m^3)], \quad s_j = \mathrm{i}\left[\frac{\omega^2}{g} - \mu_j + \beta_{j1}m + \beta_{j2}m^2 + O(m^3)\right], \tag{4.12}$$

where $j = 1, 2$, $\omega^2 > g\mu_2$ and

$$\alpha_1 = \frac{2(\omega^2 - g\mu_1)(\omega^2 - g\mu_2)}{\omega^2(\omega^2 - g^2/c_2^2)}, \quad \beta_{j1} = \frac{2(\omega^2 - N_j^2)(\omega^2 - g\mu_{3-j})}{g(\omega^2 - g^2/c_2^2)}, \tag{4.13}$$

$$\alpha_2 = \frac{(\omega^2 - g\mu_2)^2}{(\omega^2 - g^2/c_2^2)^2}\left(2 - \frac{g^2\mu_1^2}{\omega^4} - \frac{N_1^2}{\omega^2}\right) - \frac{(\omega^2 - N_2^2)^2(\omega^2 - g\mu_1)^2}{\omega^2(\omega^2 - g^2/c_2^2)^3}, \tag{4.14}$$

$$\beta_{j2} = \frac{\omega^2(\omega^2 - N_j^2)(\alpha_1^2 + 4\alpha_2) - g^2\beta_{j1}^2}{2g(\omega^2 - g\mu_j)}. \tag{4.15}$$

Coefficients (4.13)–(4.15) are singular at $\omega = \omega_0 \equiv g/c_2$, and the power expansions (4.12) are not applicable at $\omega \approx \omega_0$. This frequency range is considered separately in § 4.4. The coefficients, including β_{22}, have no other singularities at $\omega^2 \geqslant g\mu_2$. In the particular case where $c_{1,2} \to \infty$ and $\mu_{1,2} \to 0$, the approximate dispersion relation (4.12) agrees with the exact dispersion relation $\omega^2 = gq(1-m)/(1+m)$ (Lamb 1932) of the surface gravity wave propagating along an interface of two incompressible, homogeneous fluids. It is easy to check that (4.12)–(4.15) reduce to the expansions in powers of m of the explicit dispersion relation (4.7*a*) of surface AGW in the particular case where $c_1 = c_2$ and $\mu_1 = \mu_2$.

According to (4.12), $\operatorname{Im} s_1 > 0$ in the whole frequency range $\omega^2 > g\mu_2$ considered. However, at $\omega^2 = g\mu_2$, according to (4.12) and (4.13), $\beta_{21} < 0$ and $\operatorname{Im} s_2 < 0$. Hence, the requirement $\operatorname{Im} s_2 > 0$ is met, and the interface wave (4.12) exists only at frequencies $\omega > \omega_c^{(3)}$, where

$$\omega_c^{(3)} = \sqrt{g\mu_2}\left[1 + m\frac{\mu_2 - \mu_1}{\mu_2} + O(m^2)\right] \tag{4.16}$$

according to (4.12) and (4.13). The expression (4.16) for the cutoff frequency can also be obtained from (4.6) (with $j = 2$). No modified surface gravity wave exists at $\sqrt{g\mu_2} = \omega_c^{(2)} < \omega < \omega_c^{(3)}$. Note also that, according to (4.12), the effect of the upper (gas) half-space on the phase and group speeds of the interface wave is of the second order in m around the cutoff frequency $\omega_c^{(3)}$ and of the first order away from the cutoff frequency.

As we will see below, the existence of two close cutoff frequencies of the interface wave, $\omega_c^{(2)}$ and $\omega_c^{(3)}$, has a profound effect on the AGW transmission through the interface.

4.3. *Modified Lamb wave at a gas–liquid interface*

To determine the effect of the lower (liquid) half-space on the Lamb wave (4.9), we search for a solution to the general dispersion equation (4.5) in terms of an expansion in powers of m that reduces to (4.9) at $m = 0$, and obtain

$$q = \frac{\omega}{c_2}\left[1 + \nu_1 m + \nu_2 m^2 + O(m^3)\right], \quad s_j = i\left[a_j + \frac{\omega^2 - N_j^2}{a_j c_2^2}\nu_1 m + \nu_{j2}m^2 + O(m^3)\right], \tag{4.17}$$

where $j = 1, 2$, and

$$a_1 = \sqrt{\mu_1^2 - \frac{\omega^2}{c_1^2} + \frac{\omega^2 - N_1^2}{c_2^2}}, \quad a_2 = \frac{g}{c_2^2} - \mu_2, \quad \nu_1 = \frac{(\mu_1 - gc_1^{-2} - a_1)(g - \mu_2 c_2^2)}{\omega^2 - g(\mu_1 + a_1)}, \tag{4.18}$$

$$\nu_2 = \frac{\nu_1^2}{c_2^2}\left[\frac{\omega^2 - N_2^2 + g^2c_2^{-2} - \mu_2^2c_2^2}{2\left(gc_2^{-2} - \mu_2\right)^2} + \frac{2\left(\omega^2 - N_1^2\right)^2}{a_1(\omega^2 - g\mu_1 - ga_1)(\mu_1 + a_1 - N_1^2/g)}\right], \tag{4.19}$$

$$\nu_{j2} = \frac{\omega^2 - N_j^2}{2a_j^3c_2^4}\left[(\nu_1^2 + 2\nu_2)a_j^2c_2^2 - \nu_1^2(\omega^2 - N_j^2)\right]. \tag{4.20}$$

We assume for simplicity that $a_1^2 > 0$ (otherwise, the modified Lamb surface wave does not exist) and $c_2 \leqslant c_1$. Coefficients (4.18)–(4.20) are singular when $a_1 = \omega^2/g - \mu_1$ (compare with (4.8)), which corresponds to the dispersion curves of the modified Lamb and gravity waves closely approaching each other. This case is considered separately in § 4.4. It is easy to check that (4.17)–(4.20) reduce to the expansions in powers of m of the explicit dispersion relation (4.7*a*) of the surface AGW in the particular case where $c_1 = c_2$ and $\mu_1 = \mu_2$.

The phase speed of the surface wave is supersonic when $\nu_1 < 0$ and subsonic when $\nu_1 > 0$; see (4.17). It follows from (4.10) and (4.18) that ν_1 changes sign at $\omega = g/c_2$ and becomes negative at $\omega > g/c_2$. According to (4.17), $\operatorname{Im} s_1$ remains positive while $\operatorname{Im} s_2$ changes sign and becomes negative at high frequencies. The condition $\operatorname{Im} s_2 > 0$ is satisfied and the modified Lamb wave exists only at $\omega < \omega_c^{(4)}$. From (4.17)–(4.20), for the cutoff frequency we find

$$\omega_c^{(4)} = \frac{gc_2^{-2} - \mu_2}{m\sqrt{c_2^{-2} - c_1^{-2}}} - \frac{gc_2^{-2} - \mu_1}{\sqrt{c_2^{-2} - c_1^{-2}}} + O(m^2). \tag{4.21}$$

The same result is easily derived from the explicit (4.6) for cutoff frequencies (with $j = 2$) by searching for a solution that tends to infinity at $m \to 0$. Thus, unlike the Lamb wave over a rigid surface, the modified Lamb surface wave is not supported by the gas–liquid interface at high frequencies. Results similar to (4.21) have been reported earlier for a particular case where $\mu_1 = 0$ (Gasilova *et al.* 1992; Petukhov 1992). Note that $\omega_c^{(4)}$ is $O(m^{-1})$, and therefore much larger than $\omega_c^{(1,2,3)}$ and the other characteristic frequencies in the problem at hand. For orientation, the upper cutoff frequency (4.21) of the modified Lamb wave is ∼1.1 Hz at the water–air interface.

4.4. *Hybridization of the interface waves*

When $m \to 0$, the dispersion curves of the surface gravity (4.8) and Lamb (4.9) waves intersect when $\omega = \omega_0 \equiv g/c_2$; the approximate dispersion relations (4.12) and (4.17) of the modified surface gravity and Lamb waves are singular at this frequency. Physically, this reflects the fact that the fluid motion in the two surface waves becomes nearly indistinguishable. Mathematically, the singularity arises because the zeros of the two factors on the left-hand side of the dispersion equation (4.5) approach each other and coincide when $\omega = \omega_0$. The singularity suggests that developments of the dispersion relations $q(\omega, m)$ in integer powers of m do not exist at $\omega \approx \omega_0$. To find the dispersion relations of the surface waves in the frequency band where $|1 - \omega/\omega_0| \ll 1$, we approximate s_j, $j = 1, 2$, in (4.5) as follows: $s_j(q) = s_j(q_j) + [\partial s_j(q_j)/\partial q](q - q_j) + O((q - q_j)^2)$, where $q_1 = \omega^2/g$ and $q_2 = \omega/c_2$. Retaining only the terms of leading order in the small quantities $(q - q_j)$ and m, from (3.4) and (4.5) we obtain the quadratic equation:

$$(q - q_1)(q - q_2) = mb, \quad b = \frac{\omega c_2}{g^2}\left(\frac{g}{c_2^2} - \mu_2\right)(\omega^2 - g\mu_1). \tag{4.22}$$

Its solutions

$$q_s = \tfrac{1}{2}\left[q_1 + q_2 + \sqrt{(q_1 - q_2)^2 + 4mb}\right], \quad q_f = \tfrac{1}{2}\left[q_1 + q_2 - \sqrt{(q_1 - q_2)^2 + 4mb}\right] \tag{4.23}$$

define the dispersion equation of two surface waves, to be referred to as the slow and fast wave, respectively. Since $q_s > q_f$, the phase speed of the fast wave is always

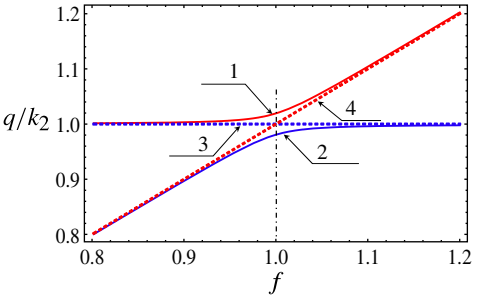

FIGURE 3. (Colour online) Dispersion curves of surface acoustic-gravity waves: (1) slow and (2) fast waves supported by a gas–liquid interface, (3) Lamb wave in a gas half-space with a rigid boundary, and (4) surface gravity wave in a liquid half-space with a free boundary. The wavenumbers of all surface waves are normalized by the wavenumber $k_2 = gc_2^{-2}f$ of the Lamb wave. Dimensionless frequency $f = \omega/\omega_0$.

higher than the phase speed of the slow wave. Higher-order terms in the dispersion equations of the slow and fast waves can be obtained by substituting (4.23) into the right-hand side of the exact equation

$$\left(1-\frac{N_1^2}{\omega^2}\right)\left(1-\frac{N_2^2}{\omega^2}\right)\left(q^2-\frac{\omega^2}{c_2^2}\right)\left(q^2-\frac{\omega^4}{g^2}\right)=m\left(\frac{N_1^2}{g}-\mu_1-|s_1|\right)$$
$$\times\left(\frac{N_2^2}{g}-\mu_2-|s_2|\right)\left(\frac{\omega^2}{g}-\mu_1+|s_1|\right)\left(\frac{\omega^2}{g}-\mu_2+|s_2|\right) \tag{4.24}$$

that follows from (3.4) and (4.5). In particular, at $\omega=\omega_0$ one finds

$$q_{s,f}=\frac{g}{c_2^2}\pm\sqrt{m\left(\frac{g}{c_2^2}-\mu_1\right)\left(\frac{g}{c_2^2}-\mu_2\right)+\frac{m}{4(gc_2^{-2}-\mu_1)}\left[\frac{g}{c_2^2}\left(\frac{5g}{c_2^2}-8\mu_1-\mu_2\right)\right.}$$
$$\left.+\frac{g}{c_1^2}\left(\frac{g}{c_2^2}-\mu_2\right)+2\mu_1^2\left(1+\frac{\mu_2c_2^2}{g}\right)\right]+O(m^{3/2}). \tag{4.25}$$

The dispersion curves of the slow and fast waves approach each other when $q_1-q_2\to 0$, i.e. $\omega\to\omega_0$ (figure 3). At the point of closest approach, the distance between the dispersion curves and, hence, the difference between the phase speeds of the surface waves are proportional to $m^{1/2}$. On the other hand, when $|\omega-\omega_0|\gg c_2\,(mb)^{1/2}$, the square root in (4.23) can be replaced by $|q_1-q_2|\lfloor 1+2mb\,(q_1-q_2)^{-2}\rfloor$. Then, at $\omega>\omega_0$, q_s in (4.23) reduces to the dispersion equation (4.12) of the modified surface gravity wave, while q_f in (4.23) reduces to the dispersion equation (4.17) of the modified Lamb wave. At $\omega<\omega_0$, q_f in (4.23) reduces to the dispersion equation (4.12) of the modified surface gravity wave, while q_s in (4.23) reduces to the dispersion equation (4.17) of the modified Lamb wave. In all four cases, (4.23) agrees with (4.12) and (4.17) up to terms $O(m^2)$.

Thus, the fast and slow surface waves are hybrids of the modified gravity and Lamb surface waves. Equation (4.23) describes the 'hybridization' of these waves around the frequency $\omega=\omega_0$, where the modified Lamb wave strongly penetrates from the gas half-space into the liquid, the modified surface gravity wave strongly penetrates from the liquid half-space into the gas, and the two surface waves become nearly indistinguishable.

Note that the approximate dispersion equation (4.23), which has been obtained in the vicinity of $\omega = \omega_0$, and the approximate dispersion equations (4.12) and (4.17), which hold away from $\omega = \omega_0$, have an overlapping domain of validity at $c_2\,(mb)^{1/2} \ll |\omega - \omega_0| \ll \omega_0$, and together give dispersion relations of surface gravity waves for all ω as long as $m \ll 1$.

4.5. *Generation of interface waves by a point source*

A point source excites only those surface waves whose poles in the integral representations (4.3) and (4.4) contribute to the respective integrals over complex q. From the requirement that a wave field due to a point source is causal, it follows that these are the poles that shift from the real axis into the upper half-plane of the complex variable q when an infinitesimal, positive imaginary part is added to the frequency ω (Brekhovskikh & Godin 1999). The modified surface gravity and Lamb waves satisfy this requirement. By calculating the residues in a corresponding pole $q = q_S$ in (4.3) and (4.4), for the field of an interface wave generated by the point source, we find

$$P_S(\boldsymbol{R}, z_0) = -0.5\mathrm{i}\omega^2 \mathrm{e}^{(\mu_1 + |s_1(q_S)|)z_0} H_0^{(1)}(q_S r) p_S(q_S, z), \tag{4.26}$$

where the vertical structure of the surface wave field is given by

$$p_S(q, z) = \frac{(\omega^2 - N_1^2)(\mu_2 - |s_2| - N_2^2/g)}{(\mu_1 + |s_1| - N_1^2/g)D'} \mathrm{e}^{(|s_1| - \mu_1)z}, \quad z < 0, \tag{4.27a}$$

$$p_S(q, z) = \frac{m}{D'}(\omega^2 - N_2^2)\mathrm{e}^{-(|s_2| + \mu_2)z}, \quad z > 0, \tag{4.27b}$$

with

$$D' \equiv \frac{\omega^2}{\mathrm{i}q}\frac{\partial D_-}{\partial q} = \frac{\omega^2 - N_2^2}{|s_2|}[\omega^2 - mN_1^2 - g(1-m)(|s_1| + \mu_1)] + \frac{\omega^2 - N_1^2}{|s_1|}[m\omega^2 - N_2^2 - g(1-m)(|s_2| - \mu_2)]. \tag{4.28}$$

Note that $D' \to \infty$ and the pressure in the surface wave becomes zero at the cutoff frequencies. In (4.26) and (4.27) and below, we use subscript S for the quantities that refer to the field of a surface wave generated by a point source.

When the appropriate dispersion equations are substituted into (4.26)–(4.28), one obtains the fields of fast and slow surface waves. In particular, for the modified surface gravity wave, $q_S = \omega^2/g$ in the frequency range (4.11), and we obtain a simple, exact result:

$$p_S(q_S, z) = \frac{\rho(z)|s_1||s_2|\exp(\omega^2 z/g)}{\rho_{10}(\omega^2 - N_1^2)(m|s_1| + |s_2|)}. \tag{4.29}$$

Together with the density profile $\rho(z)$, the pressure in the surface wave is discontinuous at the interface and varies exponentially in the gas and in the liquid. Using an approximate dispersion relation (4.12) at frequencies $\omega > \omega_c^{(3)}$ (excluding a narrow vicinity of $\omega = \omega_0$), one obtains from (4.26)–(4.28) the field of the modified surface gravity wave with accuracy to the factor $1 + O(m^3)$. To the first order in m, the vertical dependence of p_s is again given by $\rho(z)\exp(\omega^2 z/g)$ as in (4.29). The leading order of the asymptotic expansions in powers of m of the pressure amplitude on the

interface is

$$p_S|_{z=-0} = \frac{|s_1||s_2|/(\omega^2 - N_1^2)}{m|s_1|\,(\omega^2 - N_2^2)^2\,(\omega^2 - g^2/c_2^2)^{-2} + |s_2|}, \quad p_S|_{z=+0} = \frac{-m(\omega^2 - N_2^2)}{\omega^2 - g^2/c_2^2} p_S|_{z=-0}. \tag{4.30}$$

Substitution of the approximate dispersion equation (4.17) into (4.26)–(4.28) gives the field of the modified Lamb wave with accuracy to the factor $1 + O(m^3)$ (excluding a narrow vicinity of $\omega = \omega_0$). To the leading order in m, the vertical dependence of the field of the modified Lamb wave is

$$p_S = \frac{m(\omega^2 - N_1^2)|s_2|\exp((a_1 - \mu_1)z)}{2\,(\omega^2 - g\mu_1 - ga_1)^2} \quad (z < 0), \quad p_S = \frac{m|s_2|\exp(-gz/c_2^2)}{2(\omega^2 - g\mu_1 - ga_1)} \quad (z > 0). \tag{4.31}$$

Equations (4.30) and (4.31) are not applicable when $\omega - g/c_2 = O(m)$. Note that in the liquid, the pressure in the modified Lamb wave is proportional to m and is, therefore, much smaller than in the modified surface gravity wave. Since $(\omega^2 - g\mu_1 - ga_1)/(\omega^2 - g^2c_2^{-2}) = (\omega^2 - N_1^2)/(\omega^2 - g\mu_1 + ga_1) > 0$ according to (4.18), equations (4.30) and (4.31) show that the polarity of the pressure in the liquid in each surface wave changes at $\omega \approx \omega_0$. The pressures in the gas and liquid in the modified gravity (Lamb) wave are in phase at $\omega < \omega_0$ (correspondingly, $\omega > \omega_0$). That the polarity change at $z < 0$ occurs simultaneously in the two surface waves is necessary to satisfy the orthogonality relation

$$\int_{-\infty}^{+\infty} \frac{\mathrm{d}z}{\rho(z)} p_S(q_s, z) p_S(q_f, z) = 0, \tag{4.32}$$

which follows from the general theory (Godin 2012*b*) of AGW normal modes in layered fluids.

In the vicinity of $\omega = \omega_0$ (specifically, at frequencies $\omega = \omega_0 + O(c_2\,(mb)^{1/2})$), where the hybridization of the modified Lamb and surface gravity waves takes place, the amplitudes of the slow and fast surface waves become very close; the dominant terms of their asymptotic developments coincide. The analytic calculation of the subdominant terms requires expansions of the solutions q_s and q_f of the dispersion equation to second order in the small parameters. Using (4.25), at $\omega = \omega_0$ from (4.27*a*) and (4.27*b*) we find

$$\begin{aligned} p_S = {} & \frac{(gc_2^{-2} - \mu_1)}{2(g^2c_2^{-2} - N_1^2)} \\ & \times \exp\left[\left(\frac{g}{c_2^2} - 2\mu_1 \pm \left(\frac{g}{c_1^2} + \frac{g}{c_2^2} - 2\mu_1\right)\sqrt{m\frac{gc_2^{-2} - \mu_2}{gc_2^{-2} - \mu_1}} + O(m)\right) z\right] \\ & \times \left\{1 \pm \frac{m^{1/2}}{4}\frac{(gc_2^{-2} - \mu_2)^{-1/2}}{(gc_2^{-2} - \mu_1)^{3/2}}\left[\frac{3g}{c_1^2}\left(\frac{g}{c_2^2} - \mu_2\right)\right.\right. \\ & \left.\left. + \frac{g}{c_2^2}\left(\frac{5g}{c_2^2} - 12\mu_1 - \mu_2\right) + 4\mu_1(\mu_1 + \mu_2)\right] + O(m)\right\}, \quad z < 0, \end{aligned} \tag{4.33}$$

$$p_S = \frac{\exp\left[-\left(gc_2^{-2} \pm 2\sqrt{m(gc_2^{-2}-\mu_1)(gc_2^{-2}-\mu_2)} + O(m)\right)z\right]}{2(g^2c_2^{-2}-N_1^2)} \times \left\{\mp\sqrt{m\left(\frac{g}{c_2^2}-\mu_1\right)\left(\frac{g}{c_2^2}-\mu_2\right)} - \frac{m}{2(gc_2^{-2}-\mu_1)}\left[\frac{g}{c_1^2}\left(\frac{g}{c_2^2}-\mu_2\right) + \frac{g}{c_2^2}\left(\frac{3g}{c_2^2}-6\mu_1-\mu_2\right) + 2\mu_1(\mu_1+\mu_2)\right] + O(m^{3/2})\right\}, \quad z>0. \tag{4.34}$$

Here, as in (4.25), the upper (lower) sign refers to the slow (fast) surface wave, respectively. Compared to the equations (4.29)–(4.31) for pressure in the surface waves away from the hybridization frequency $\omega = \omega_0$ and the cutoff frequencies, equation (4.34) predicts amplification of the pressure in the gas by the large factor $O(m^{-1/2})$ in the vicinity of the hybridization frequency. When the pressure and, consequently, the horizontal displacement are amplified, the vertical displacement in the surface waves remains a quantity $O(m^0)$ according to (3.3), (4.25), (4.33) and (4.34).

The fast and slow surface waves have rather similar surface amplitudes and vertical profiles, and their interference leads to strong modulation of the AGW field at frequencies close to the hybridization frequency $\omega = \omega_0$. The spatial period of the interference pattern, $2\pi/(q_s - q_f)$, which is generally of the order of the AGW wavelength, increases by a factor $O(m^{-1/2})$ and becomes very large when $\omega - \omega_0 = O(m)$ (see (4.23)). At $\omega = \omega_0$ and $r \ll m^{-1/2}g^{-1}c_2^2$, the pressure fields due to the fast and slow surface waves interfere constructively in the liquid and destructively in the gas, so that the pressure due to the surface waves in the gas is $O(m)$ and is not appreciably amplified compared to the pressure at frequencies away from $\omega = \omega_0$. Thus, the pressure amplification predicted by (4.34) is observed only at horizontal separations $r \sim m^{-1/2}g^{-1}c_2^2$ and greater from the source.

5. Wave energy radiated by a point source

Consider a right cylinder $\{-H < z < H,\ 0 \leqslant r < r_C\}$, where $H > -z_0$. The cylinder contains the point source located in the liquid, and therefore the power flux through the surface of the cylinder gives the total power J_T radiated by the source. Generally, both body waves (the continuous spectrum of the problem) and surface waves (the discrete spectrum of the problem) contribute to the field and power flux at each point of the surface of the cylinder. When $r_C \to \infty$, the power flux through the lateral surface $\{-H < z < H,\ r = r_C\}$ of the cylinder is solely due to the surface waves since the contributions of the body waves attenuate as r_C^{-1} or faster (Brekhovskikh & Godin 1999). When $H \to \infty$, the power flux through the bases $\{z = \pm H,\ 0 \leqslant r < r_C\}$ of the cylinder is solely due to the propagating plane waves in the continuous spectrum, since the evanescent waves and the surface waves attenuate exponentially with H. Thus, the AGW power flux J_G radiated into the gas can be calculated as the sum of the power flux J_{G1} due to the propagating plane waves through the upper base of a sufficiently large cylinder and the power flux J_{G2} due to the surface waves through the lateral surface of the cylinder in the upper half-space. Similarly, the AGW power flux J_L radiated to infinity within the liquid equals the sum of the power flux J_{L1} due to the propagating plane waves through the lower base of the cylinder and the power

flux J_{L2} due to the surface waves through the lateral surface of the cylinder in the lower half-space.

5.1. *Power carried to infinity by body waves*

According to (3.4), the propagating plane waves (i.e. plane waves with $\operatorname{Im} s_j = 0$) have wavenumbers $0 \leqslant q \leqslant q^{(j)}$, where

$$q^{(j)} = \frac{\omega}{c_j}\sqrt{\frac{\omega^2 - \mu_j^2 c_j^2}{\omega^2 - N_j^2}} \tag{5.1}$$

and $j = 1$ and 2 for the gas and liquid, respectively. The pressure due to propagating plane waves generated by a point source of volume velocity is given by (2.7), (4.3) and (4.4), where $\boldsymbol{F} = 0$ and integration is restricted to the interval $-q^{(j)} < q < q^{(j)}$. Using (3.2) and (3.3) and integrating the vertical component of the power flux density $\boldsymbol{I}$ in (3.5) over the plane $z = H$, for the power flux to infinity due to the propagating plane waves in the gas we find

$$J_{G1} = \frac{|A_0^2|\rho_1(z_0)\,(\omega^2 - N_1^2)^2}{16\pi m\omega\,(\omega^2 - N_2^2)} \int_0^{q^{(2)}} \left|\frac{W}{s_1}\right|^2 s_2 \mathrm{e}^{2z_0 \operatorname{Im} s_1} q\,\mathrm{d}q. \tag{5.2}$$

Derivation of (5.2) is simplified if one chooses in (4.4) the representation of the wave field as an integral over plane rather than cylindrical waves.

Quite similarly, by integrating the vertical component of the power flux density $\boldsymbol{I}$ in (3.5) over the plane $z = -H$, for the power flux to infinity due to the propagating plane waves in the liquid we obtain

$$J_{L1} = \frac{|A_0^2|\rho_1(z_0)}{16\pi\omega}(\omega^2 - N_1^2) \int_0^{q^{(1)}} \frac{q\,\mathrm{d}q}{s_1} |1 + V\mathrm{e}^{-2\mathrm{i}s_1 z_0}|^2. \tag{5.3}$$

Note that the power fluxes due to the propagating plane waves through the planes $z = \pm H$ are independent of H. Equations (5.2) and (5.3) show that plane (or cylindrical) waves with different wavenumbers q make additive contributions to the radiated power.

The boundary conditions (2.3) ensure that the normal component of the power flux density $\boldsymbol{I}$ in (3.5) is continuous at the fluid–fluid interface. Since J_{G1} is independent of H for all $H > 0$, the power flux can be calculated as the vertical power flux in the liquid at $z = -0$. This leads to the expression

$$J_{G1} = \frac{|A_0^2|\rho_1(z_0)}{16\pi\omega}(\omega^2 - N_1^2)\operatorname{Re} \int_0^{q^{(2)}} \frac{q\,\mathrm{d}q}{s_1}\,(1 - |V|^2 + 2\mathrm{i}\operatorname{Im} V)\mathrm{e}^{2z_0 \operatorname{Im} s_1}. \tag{5.4}$$

Equations (5.3) and (5.4) differ from the corresponding results for acoustic waves (Godin 2006*b*) only by the presence of N_1^2, by the upper limits of integration, and by the different dependences of $s_{1,2}$ and V on q. While only propagating plane waves in the liquid contribute to J_{L1}, both propagating plane waves and those evanescent plane waves in the liquid that become propagating plane waves in the gas after refraction at the interface contribute to J_{G1}. The contribution of the evanescent waves is described by the term $2\mathrm{i}\operatorname{Im} V$ in brackets in the integrand in (5.4). The frequency range at which the evanescent waves contribute to J_{G1} is determined from the inequality $q^{(1)}(\omega) < q^{(2)}(\omega)$. Aside from the common factor $\rho_1(z_0)$ in the right-hand side of (5.4), the contribution of the propagating plane waves in the liquid to J_{G1} is independent of the source position, while the contribution of the evanescent waves

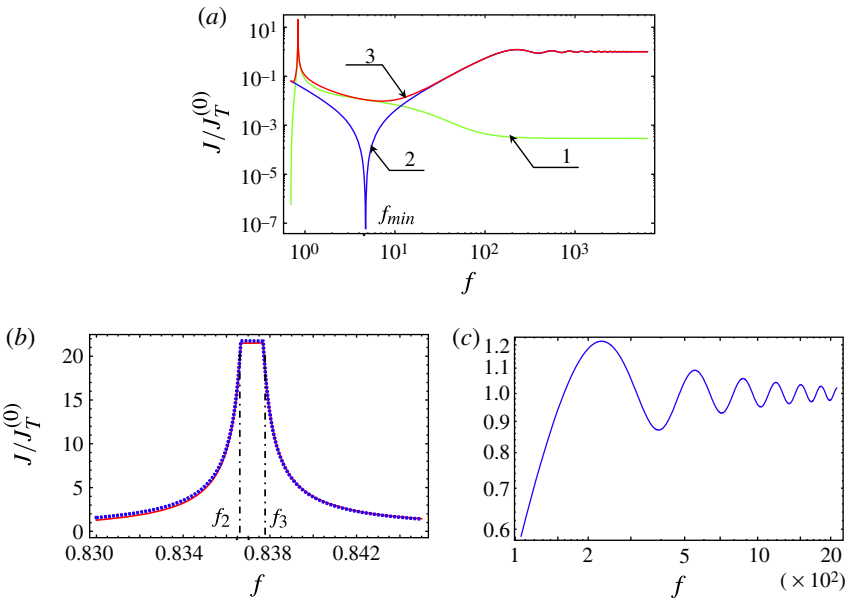

FIGURE 4. (Colour online) Power fluxes carried from a point source by body waves. (*a*) Power fluxes radiated to infinity within the gas, J_{G1} (1), and within the liquid, J_{L1} (2), and the total power flux carried by body waves (3). (*b*) Numerical evaluation (solid line) and analytic approximation (5.11) (dashed line) of the power flux into gas, J_{G1}, in the vicinity of its maximum. (*c*) Power radiated to infinity within the liquid at high frequencies. Source depth $|z_0| = 500$ m. All power fluxes are normalized by the power $J_T^{(0)}$ radiated by the source into unbounded liquid (see (5.5)). Dimensionless frequency $f = \omega/\omega_0$, $f_{min} = g^{1/2}/|z_0|^{1/2}\,\omega_0$, $f_j = \omega_c^{(j)}/\omega_0$, where $j = 2, 3$ and $\omega_c^{(2)}$ and $\omega_c^{(3)}$ are cutoff frequencies of the modified surface gravity wave.

decreases steadily with the source depth because of the factor $\exp(2z_0 \operatorname{Im} s_1)$ in the integrand. On the other hand, the power flux J_{L1} (5.3) to infinity in the liquid has a non-monotonic dependence on z_0 and wave frequency because of the interference of the direct and interface-reflected propagating plane waves with the same q (figure 4). The interference is described by the factor $|1 + V\mathrm{e}^{-2is_1 z_0}|^2$ in the integrand in (5.3). Power flux J_{L1} has a deep minimum (figure 4*a*), which is caused by the destructive interference of the direct and reflected waves that occurs in a wide range of q values at $\omega \approx (g/|z_0|)^{1/2}$ (Fuks & Godin 2011).

In the particular case where the same fluid occupies half-spaces $z < 0$ and $z > 0$, the reflection coefficient $V = 0$ and there are no surface waves. Then the total power output of the point source equals $J_{L1} + J_{G1}$, and for the power radiated by the source in an unbounded liquid from (5.1), (5.3) and (5.4) we find

$$J_T^{(0)} = \frac{\omega |A_0^2| \rho_1(z_0)}{8\pi} \sqrt{\frac{\omega^2}{c_1^2} - \mu_1^2}. \tag{5.5}$$

Using (3.7) and (5.2), one obtains

$$J_{G1} = \frac{|A_0^2| m \rho_1(z_0)}{4\pi\omega} (\omega^2 - N_1^2)^2 (\omega^2 - N_2^2) \int_0^{q^{(2)}} s_2 \mathrm{e}^{2z_0 \operatorname{Im} s_1} \frac{q\,\mathrm{d}q}{|D_-^2|}. \tag{5.6}$$

As a function of source depth, J_{G1} tends to its minimum value $J_G^{(0)}$ when $z_0 \to -\infty$; $J_G^{(0)}$ has the meaning of the total power radiated into the gas by a very deep source. After some algebra, from (3.8), (5.5) and (5.6) we find

$$\begin{aligned} J_G^{(0)} &= \frac{|A_0^2|m\rho_1(z_0)}{4\pi\omega}\,(\omega^2 - N_1^2)^2(\omega^2 - N_2^2)\int_0^{q^{(1)}} s_2 \frac{q\,\mathrm{d}q}{|D_-^2|} \\ &= \frac{2m(\omega^2 - N_1^2)J_T^{(0)}\,[1 + O(m)]}{(\omega^2 - g^2c_2^{-2})\sqrt{\omega^2c_1^{-2} - \mu_1^2}} \\ &\quad \times \left[S_1\left(\arctan\frac{S_2}{S_1} - \arctan\frac{S_3}{S_1}\right) - \left(\frac{N_2^2}{g} - \mu_2\right)\right. \\ &\quad \left. \times \left(\arctan\frac{gS_2}{N_2^2 - g\mu_2} - \arctan\frac{gS_3}{N_2^2 - g\mu_2}\right)\right], \end{aligned} \tag{5.7}$$

where $S_1 \equiv \omega^2/g - \mu_2$, $S_2 \equiv s_2(q=0) = \sqrt{\omega^2c_2^{-2} - \mu_2^2}$ and $S_3 \equiv s_2(q = q^{(1)}) = \sqrt{\omega^2c_2^{-2} - \mu_2^2 - (\omega^2c_1^{-2} - \mu_1^2)(\omega^2 - N_2^2)/(\omega^2 - N_1^2)}$. The power flux $J_G^{(0)}$ in (5.7) is always non-negative and has no singularities at $\omega = (g\mu_2)^{1/2}$ and $\omega = g/c_2$.

Generally, D_- in (3.8) is $O(m^0)$, and therefore $J_{G1} = O(m)$ for arbitrary z_0. Then, the power J_{G1} transmitted into the gas is small compared to the power $J_T^{(0)}$ in (5.5) radiated into an unbounded liquid, but is not necessarily small compared to the power J_{L1} radiated to infinity in the liquid. A large increase in the power flux into the gas is expected in special cases, where D_- becomes small. The dominant term $O(m^0)$ in D_- vanishes when either $s_2 = O(m)$ and $N_2^2 = g\mu_2$ (a situation that is impossible in any isothermal perfect gas) or $\omega^2 - g\mu_1 + \mathrm{i}gs_1 = O(m)$ (which becomes possible at $q \approx \omega^2/g$ for frequencies $\omega^2 \approx g\mu_2$). The latter possibility is investigated below.

Consider AGWs with frequencies close to $(g\mu_2)^{1/2}$. Then, $|S_1| \ll \mu_2$. According to (3.4), s_2 in propagating plane waves in the gas takes values $0 \leqslant s_2 \leqslant S_2$. When s_2 is small, the corresponding plane waves in the liquid (i.e. plane waves with the same q) are evanescent: $s_1 = \mathrm{i}|s_1|$, $|s_1| = \omega^2/g - \mu_1 + O(s_2^2/S_2)$. Neglecting terms of the fifth and higher orders in the small parameters s_2, S_1 and m, from (3.4) and (3.8) we obtain

$$|D_-^2| = \frac{(\omega^2 - N_1^2)^2}{4\,(\mu_2 - \mu_1)^2}(S_1^2 + s_2^2)\{[2m(\mu_2 - \mu_1) - S_1]^2 + s_2^2\} + O((|S_1| + s_2 + m)^5). \tag{5.8}$$

Equation (5.8) is consistent with the results of § 4.2, where it was shown that D_- has zeros at $s_2 = -\mathrm{i}S_1$ (when $S_1 < 0$) and at $s_2 \approx \mathrm{i}[S_1 + 2m(\mu_1 - \mu_2)]$ (when $0 < S_1 \ll \mu_2$); see (4.12) and (4.13). For the leading order of the asymptotic expansion of J_{G1} in powers of S_1 and m, from (5.6) and (5.8) we obtain

$$J_{G1} = \pi^{-1}|A_0^2|m\omega\rho_1(z_0)\,(\mu_2 - \mu_1)^2\exp(2z_0(\mu_2 - \mu_1))\Psi(2m(\mu_2 - \mu_1) - S_1), \tag{5.9}$$

where

$$\Psi(\chi) \equiv \int_0^{S_2} \frac{s_2^2\,\mathrm{d}s_2}{(S_1^2 + s_2^2)(\chi^2 + s_2^2)} = \frac{1}{S_1^2 - \chi^2}\left[|S_1|\arctan\left(\frac{S_2}{|S_1|}\right) - |\chi|\arctan\left(\frac{S_2}{|\chi|}\right)\right]. \tag{5.10}$$

Since $S_2 \gg \max[|S_1|, 2m(\mu_2 - \mu_1)]$, we replace arctangents in (5.10) with $\pi/2$ and obtain the following approximation for the power flux J_{G1}:

$$J_{G1} = |A_0^2|\omega\rho_1(z_0)(\mu_2 - \mu_1)\mathrm{e}^{2z_0(\mu_2-\mu_1)}\frac{|2m(\mu_2 - \mu_1) + \mu_2 - \omega^2/g| - |\mu_2 - \omega^2/g|}{8[m(\mu_2 - \mu_1) + \mu_2 - \omega^2/g]}. \tag{5.11}$$

Equation (5.11) agrees with numerical evaluation of the integral (5.2) and describes a high, narrow peak in the frequency dependence of the power flux J_{G1} into gas (figure 4*b*). The peak has an unusual, flat top (plateau) at $0 \leqslant \omega^2 - g\mu_2 \leqslant 2mg(\mu_2 - \mu_1)$, with the maximum of the power flux exceeding the values of J_{G1} far from $\omega^2 = g\mu_2$ by a factor $O(m^{-1})$. In terms of the cutoff frequencies of the modified gravity wave, considered in § 4.2, the plateau is located at $\omega_c^{(2)} \leqslant \omega \leqslant \omega_c^{(3)}$. The width of the plateau and the frequency scale of the J_{G1} decrease away from the plateau are proportional to m. The drastic increase at $\omega^2 \approx g\mu_2$ of the power flux J_{G1} due to the propagating plane waves in the gas occurs because the reflection and transmission coefficients (3.7) acquire very large absolute values at $q \approx \omega^2/g$. Note that the increase in J_{G1} is not accompanied by an increase or any peculiarities of the power flux J_{L1} to infinity in the liquid, since the plane waves in the liquid, unlike in the gas, are evanescent when $\omega^2 \approx g\mu_2$ and $q \approx \omega^2/g$.

5.2. *Power fluxes in surface waves*

Consider a power flux carried by an individual surface wave (4.26). By integrating the flux of vector $\boldsymbol{I}$ in (3.5) through the cylindrical surface $r = r_C$ at $0 < z < \infty$ and $-\infty < z < 0$, for the power fluxes J_{GS} and J_{LS} in the gas and in the liquid, we find from (2.7), (4.26) and (4.27) that

$$J_{GS} = \frac{|A_0^2|\rho_1(z_0)\omega}{4m|s_2(q_S)|}\left(\omega^2 - N_1^2\right)^2 |p_S(q_S, z = +0)|^2 \exp[2z_0|s_1(q_S)|], \tag{5.12a}$$

$$J_{LS} = \frac{|A_0^2|\rho_1(z_0)\omega}{4|s_1(q_S)|}\left(\omega^2 - N_1^2\right)^2 |p_S(q_S, z = -0)|^2 \exp[2z_0|s_1(q_S)|]. \tag{5.12b}$$

In the derivation of (5.12*a*) and (5.12*b*) we took into account that the radial component of particle displacement equals $(\omega^2\rho)^{-1}\,\partial p/\partial r$ according to (2.1) and that $\mathrm{Im}\,[(H_0^{(1)}(u))^*\,\mathrm{d}H_0^{(1)}(u)/\mathrm{d}u] = 2/\pi u$ (Abramowitz & Stegun 1965, p. 360). The power fluxes are independent of the radius r_C of the cylindrical surface. The distribution of the power flux in the surface wave between the gas and liquid half-spaces is described by the concise equation

$$\frac{J_{GS}}{J_{LS}} = \frac{|s_1(q_S)|}{m|s_2(q_S)|}\left|\frac{p_S(q_S, z = +0)}{p_S(q_S, z = -0)}\right|^2. \tag{5.13}$$

General expressions for the surface wave amplitude $|p_S(q_S, z = \pm 0)|$ on the gas and liquid sides of the interface are given by (4.27) and (4.28).

In the particular case of a modified surface gravity wave, at frequencies $\omega_c^{(1)} \leqslant \omega \leqslant \omega_c^{(2)}$ from (4.29), (5.12*a*), (5.12*b*) and (5.13) we find

$$J_{Gg} = \frac{|A_0^2|\rho_1(z_0)\omega m\,|s_1|^2\,|s_2|}{4\,(m|s_1| + |s_2|)^2}\mathrm{e}^{2z_0|s_1|}, \quad J_{Lg} = J_{Gg}\frac{|s_2|}{m|s_1|}. \tag{5.14}$$

This is an exact result. Here and below, the first subscript specifies, as before, the half-space, where the energy flux is considered, while the second subscript specifies

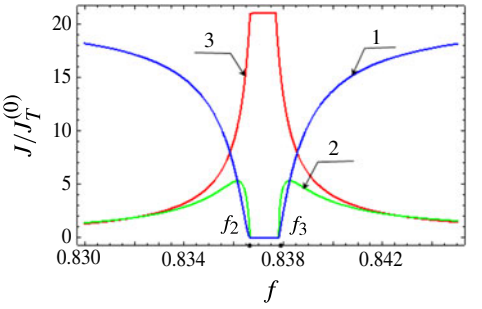

FIGURE 5. (Colour online) Power fluxes carried in liquid, J_{Lg} (1), and gas, J_{Gg} (2), half-spaces by the modified surface gravity wave. Power flux J_{G1} (3) radiated into the gas in body waves is shown for comparison. Source depth $|z_0| = 500$ m. All power fluxes are normalized by the power $J_T^{(0)}$ radiated by the source into unbounded liquid. Dimensionless frequency $f = \omega/\omega_0, f_j = \omega_c^{(j)}/\omega_0$, where $j = 2, 3$ and $\omega_c^{(2)}$ and $\omega_c^{(3)}$ are cutoff frequencies of the modified surface gravity wave.

the surface wave (g and l stand for modified gravity and Lamb waves, respectively). At frequencies $\omega \geqslant \omega_c^{(3)}$, from (4.30), (5.12*a*), (5.12*b*) and (5.13) we find asymptotically, to the leading order in m, that the power fluxes are still described by (5.14), if $|s_2|$ in (5.14) is replaced by

$$|\tilde{s}_2| = (\omega^2 - N_2^2)^{-2} (\omega^2 - g^2/c_2^2)^2 |s_2|. \tag{5.15}$$

Equations (5.14) and (5.15) show that the power fluxes in the modified gravity wave vanish, as expected, at the cutoff frequencies $\omega_c^{(j)}$, where $j = 1, 2, 3$, since $s_1 = 0$ at $\omega = \omega_c^{(1)}$ and $s_2 = 0$ at $\omega = \omega_c^{(2)}$ and $\omega = \omega_c^{(3)}$. The power flux J_{Lg} carried by the surface wave in the liquid half-space is $O(m^0)$. Depending on the sound speed in the liquid and the source depth $-z_0$, J_{Lg} can far exceed the power output $J_T^{(0)}$ (5.5) of the source in the unbounded liquid (figure 5). Except for the vicinities of the cutoff frequencies $\omega_c^{(2,3)}$, the power flux J_{Gg} carried by the surface wave in the gas half-space is $O(m)$ and is much smaller than J_{Lg}. However, when either $0 < \omega_c^{(2)} - \omega = O(m)$ or $0 < \omega - \omega_c^{(3)} = O(m)$, J_{Gg} rapidly increases and becomes a quantity $O(m^0)$; when $|s_2| < m|s_1|$, more energy is transported by the surface wave in the gas than in the liquid (figure 5).

In the case of the modified Lamb wave, at frequencies below its cutoff frequency $\omega_c^{(4)}$ in (4.21), from (4.31), (5.12*a*), (5.12*b*) and (5.13) we find asymptotically, to the leading order in m, that

$$J_{Gl} = \frac{|A_0^2|\rho_1(z_0)\omega\,(\omega^2 - N_1^2)^2\, m|s_2|}{16\,(\omega^2 - g\mu_1 - g|s_1|)^2} \mathrm{e}^{2z_0|s_1|}, \quad J_{Ll} = J_{Gl} \frac{m|s_2|\,(\omega^2 - N_1^2)^2}{|s_1|\,(\omega^2 - g\mu_1 - g|s_1|)^2}. \tag{5.16}$$

Equation (5.16) as well as (5.15) do not apply in the vicinity of the hybridization frequency $\omega = g/c_2$. According to (5.16), the power flux carried by the modified Lamb wave vanishes at $\omega = \omega_c^{(4)}$, as expected. Away from the cutoff frequency, the power flux J_{Gl} in the gas is $O(m)$, while the power flux J_{Ll} in the liquid is $O(m^2)$ and is much smaller than J_{Gl} (figure 6). Also J_{Ll} is much smaller than the power flux in the liquid in the modified gravity wave provided the product $|z_0 s_1|$ is not too large in the latter. The relative significance of the two surface waves is reversed at high frequencies,

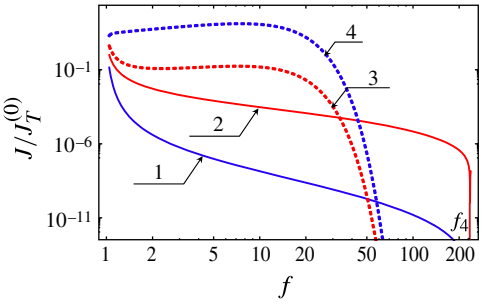

FIGURE 6. (Colour online) Power fluxes carried in the liquid, J_{Ll} (1) and J_{Lg} (4), and in the gas, J_{Gl} (2) and J_{Gg} (3), by the modified Lamb (1 and 2) and modified surface gravity (3 and 4) waves. Source depth $|z_0| = 500$ m. All power fluxes are normalized by the power $J_T^{(0)}$ radiated by the source into unbounded liquid. Dimensionless frequency $f = \omega/\omega_0$, $f_4 = \omega_c^{(4)}/\omega_0$, where $\omega_c^{(4)}$ is the cutoff frequency of the modified Lamb wave.

where the wavelength of the modified gravity wave is much smaller than that of the modified Lamb wave and is of the order of or smaller than $|z_0|$. Then, $J_{Gl} \gg J_{Gg}$ due to the rapid attenuation of the gravity wave with depth (figure 6).

The power fluxes carried by the two surface waves and their distribution between the gas and liquid half-spaces become rather similar in the vicinity $\omega - \omega_0 = O(m)$ of the hybridization frequency. At $\omega = \omega_0$, from (4.25), (4.33), (4.34), (5.12*a*) and (5.12*b*) we find

$$J_{GS} = \tilde{J}\left[1 \pm m^{1/2}\left(\frac{g}{c_2^2} - \mu_1\right)^{-3/2}\left(\frac{g}{c_2^2} - \mu_2\right)^{1/2}\left(\frac{g}{c_2^2} - \frac{N_1^2}{g}\right)\right][1 + O(m)], \quad (5.17)$$

$$J_{LS} = \tilde{J}\left[1 \pm m^{1/2}\left(\frac{g}{c_2^2} - \mu_1\right)^{1/2}\left(\frac{g}{c_2^2} - \mu_2\right)^{-1/2}\left(2 - \frac{g(gc_2^{-2} - \mu_2)(c_2^{-2} - c_1^{-2})}{2\,(gc_2^{-2} - \mu_1)^2}\right)\right] \times [1 + O(m)]. \quad (5.18)$$

Here

$$\tilde{J} = \frac{|A_0^2|\rho_1(z_0)g}{16c_2}\left(\frac{g}{c_2^2} - \mu_1\right)\exp\left[2z_0\left(\frac{g}{c_2^2} - \mu_1 \pm \sqrt{m\left(\frac{g}{c_2^2} - \mu_1\right)\left(\frac{g}{c_2^2} - \mu_2\right)}\right)\right] \quad (5.19)$$

and, as in (4.25), the upper (lower) sign refers to the slow (fast) surface wave, respectively. Note that the power fluxes in the gas far exceed their values away from the hybridization frequency and remain finite in the limit $m \to 0$ (figure 7).

The mode orthogonality relation (4.32) ensures that the total power flux carried from the source by waves in the discrete spectrum of the field is the sum of power fluxes carried by the individual surface waves. However, the power fluxes carried by the two surface waves in the gas (or liquid) half-space are not additive. By representing the discrete spectrum of the field as a sum of the fields of two surface waves (4.26) and integrating the flux of vector $\boldsymbol{I}$ in (3.5) through the cylindrical surface $r = r_C$ at $0 < z < \infty$ and $-\infty < z < 0$, for the power fluxes J_{G2} and J_{L2} in the discrete spectrum

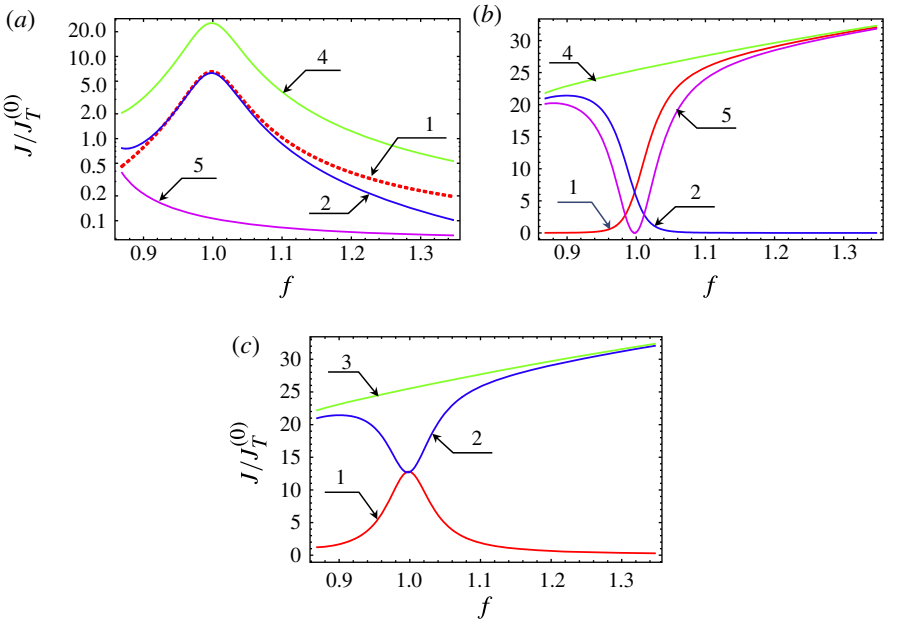

FIGURE 7. (Colour online) Power fluxes carried by interface waves (*a*) in the gas, (*b*) in the liquid, and (*c*) in the entire medium. Individual curves refer to power fluxes in the slow surface wave (1), in the fast surface wave (2), total power radiated by the source into surface waves (3), and maximum (4) and minimum (5) (with respect to r_C) power fluxes through the cylindrical surface $r = r_C$ at $0 < z < \infty$ and $-\infty < z < 0$. Source depth $|z_0| = 500$ m. All power fluxes are normalized by the power $J_T^{(0)}$ radiated by the source into unbounded liquid. Dimensionless frequency $f = \omega/\omega_0$.

in the gas and in the liquid, we find from (2.7), (4.26) and (4.27) that

$$J_{G2}(r_C) = J_{Gl} + J_{Gg} - J_{in}\cos(q_s - q_f)r, \quad J_{L2}(r_C) = J_{Ll} + J_{Lg} + J_{in}\cos(q_s - q_f)r, \tag{5.20}$$

where

$$J_{in} = \frac{2(q_s + q_f)}{|s_2(q_s)| + |s_2(q_f)|}\sqrt{\frac{|s_2(q_s)s_2(q_f)|}{q_s q_f}J_{Gg}J_{Gl}}$$
$$= \frac{2(q_s + q_f)}{|s_1(q_s)| + |s_1(q_f)|}\sqrt{\frac{|s_1(q_s)s_1(q_f)|}{q_s q_f}J_{Lg}J_{Ll}}. \tag{5.21}$$

While the total power flux through the cylindrical surface $\{r = r_C, \quad -\infty < z < \infty\}$ equals $J_{G2}(r_C) + J_{L2}(r_C) = J_{Gl} + J_{Gg} + J_{Ll} + J_{Lg}$ and is independent of r_C, the power fluxes in the gas and the liquid half-spaces are periodic functions of r_C. Variations of J_{G2} and J_{L2} with range reflect the periodic power flux through the interface, which results from the interference of the surface waves and does not happen at frequencies $\omega_c^{(2)} < \omega < \omega_c^{(3)}$ and $\omega > \omega_c^{(4)}$, when only one surface wave is supported by the interface.

The modulation of the power fluxes in the gas and liquid half-spaces by the interference of the surface waves is most pronounced at frequencies close

to the hybridization frequency, where the power fluxes in the individual surface waves become very close. According to (4.25), (5.17), (5.18), (5.20) and (5.21), $\max J_{G2} = O(m^0)$, $\min J_{G2} = O(m^{1/2})$, $\max J_{L2} = O(m^0)$ and $\min J_{L2} = O(m^{1/2})$ at $\omega = \omega_0$. Note that, with the increasing radius of the cylindrical surface, the power flux in the gas half-space first reaches values of $J_{G2} = O(m^0)$ at $r_C \sim m^{-1/2}\left(gc_2^{-2} - \mu_1\right)^{-1/2}\left(gc_2^{-2} - \mu_2\right)^{-1/2}$; $J_{G2} = O(m^{1/2})$ and tends to zero when $m \to 0$, for all $r_C = O(m^0)$. This could have been anticipated since the power flux in the gas should vanish in the limit $m \to 0$ for all finite r_C.

6. Discussion

An interface does much more to an AGW radiation by a compact source than simply distribute the power emitted by the source between two fluids. While the power output in an unbounded liquid, $J_T^{(0)}$ in (5.5), provides a suitable normalization for AGW power fluxes, it should be emphasized that, in the presence of a gas–liquid interface, the power output of the source as well as the power fluxes radiated to infinity in the gas and in the liquid each can be either much smaller or much larger than $J_T^{(0)}$. In particular, the power fluxes in the surface waves tend to zero when the source depth $|z_0| \to \infty$ but at moderate $|z_0|$ far exceed $J_T^{(0)}$ in a broad range of frequencies (figures 5–7). (This is similar to the role that surface waves play in the case of a source of elastic waves located in a solid half-space below a gas–solid interface (Godin 2011).) That neither the excitation of surface waves nor the AGW radiation into the gas half-space are limited by the power emitted by the same source in an unbounded liquid becomes evident if one considers the limiting case of an incompressible, homogeneous liquid. All monochromatic plane waves in such a liquid are inhomogeneous and do not carry energy away from the source. When $c_1 \to \infty$ and $\mu_1 \to 0$, one obtains $q^{(1)} = 0$ and $J_T^{(0)} = 0$ from (5.1) and (5.5), but the amplitudes of the surface waves as well as the power flux J_{G1} (5.2) in the body waves into the gas remain finite.

When the source approaches the interface, the transmitted power increases and can exceed by several orders of magnitude the power $J_G^{(0)}$ in (5.7) radiated into the gas half-space by a very deep source (figure 8). This is similar to the previously studied anomalous transparency of gas–liquid interfaces for low-frequency sound (Godin 2006*b*, 2007, 2008*b*), where the transmitted power increases dramatically when a localized sound source approaches the interface to within a fraction of the wavelength in the gas. As for sound, the AGW transmission into the gas increases with decreasing source depth due to the contribution of plane waves that are inhomogeneous in the liquid but become homogeneous plane waves in the gas upon refraction at the interface. The horizontal wavenumbers q of these waves satisfy the inequality $q^{(1)} < q < q^{(2)}$; see (5.1). Equation (5.6) shows that their contribution to the power flux into the gas far exceeds the contribution of the homogeneous plane waves in the liquid, for which $0 < q < q^{(1)}$, when $|z_0| \operatorname{Im} s_1(q^{(2)}) = O(1)$ and $q^{(1)} \ll q^{(2)}$, as is usually the case at gas–liquid interfaces.

Depending on the wave frequency and the parameters of the fluids, a large and even dominant contribution to the power flux through the interface is due to the excitation of the surface waves (figure 8*b*). This mechanism of AGW transmission has no counterpart in the acoustic problem as long as the interface is flat. This contribution is sensitive to the source depth, especially at higher frequencies, and vanishes when $|z_0| \to \infty$. The power fluxes in a surface wave tend to zero when

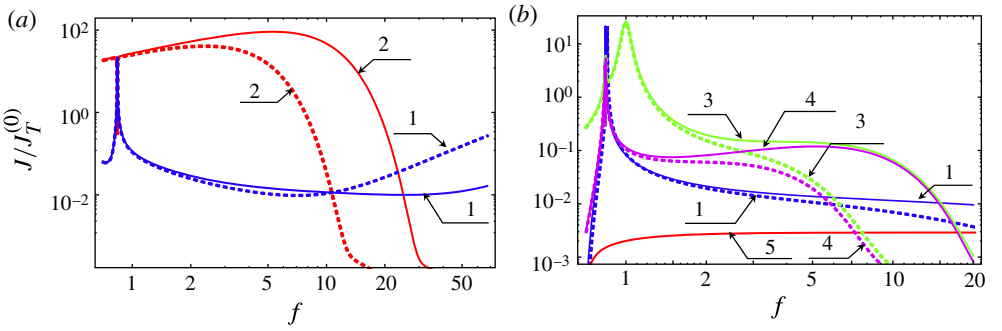

FIGURE 8. (Colour online) Power fluxes (*a*) radiated by a point source in the liquid and (*b*) transmitted into the gas. Individual curves refer to the power flux in body waves (1), the total power radiated by the source into surface waves (2), and maximum (3) and minimum (4) (with respect to r_C) power fluxes in surface waves through the cylindrical surface $r = r_C$ at $0 < z < \infty$. Source depth: $|z_0| = 100$ m (solid lines) and $|z_0| = 500$ m (dashed lines). For comparison, $10J_G^{(0)}$, i.e. ten times the power radiated into gas by a very deep source, is also shown (5). All power fluxes are normalized by the power $J_T^{(0)}$ radiated by the source into unbounded liquid. Dimensionless frequency $f = \omega/\omega_0$.

the wave frequency approaches a cutoff frequency of the surface wave. The cutoff frequencies of the modified surface gravity wave $\omega = \omega_c^{(j)}$, $j = 1, 2, 3$, are given by (4.11) and (4.16). At the water–air interface with parameters given in § 3, $\omega_c^{(1)}$ and $\omega_c^{(2)}$ correspond to ∼1 mHz (wave period ∼18 min) and 3.95 mHz (wave period 253 s), while $\omega_c^{(3)}/\omega_c^{(2)} - 1 \approx 1.3 \times 10^{-3}$. The modified Lamb wave exists at $\omega < \omega_c^{(4)}$, where the cutoff frequency $\omega_c^{(4)}$ in (4.21) corresponds to 1.12 Hz. At $\omega > \omega_c^{(4)}$, the contribution of the surface waves to the AGW transmission is negligible.

For acoustic waves, an increase of the power flux into the gas with decreasing source depth is accompanied by a destructive interference of direct and surface-reflected waves at $z < z_0$ and by a resulting near-cancellation of the sound field in the liquid (Godin 2006*b*, 2007; McDonald & Calvo 2007). While the acoustic pressure in the liquid is $O(m^0)$ for finite z_0, at $z_0 \to 0$ it becomes a quantity $O(m)$. On the contrary, the excitation of the surface waves by a compact source ensures that no such cancellation of the AGW field occurs. In terms of the plane-wave reflection coefficient V in (3.7), the lack of AGW field cancellation in the liquid follows from the fact that $\lim_{m\to 0} V \neq -1$ when $g \neq 0$, which precludes the destructive interference of direct and reflected waves at $z_0 \to 0$.

The most remarkable features of AGW transmission through gas–liquid interfaces are the resonance-like enhancements of the transmission that occur at $\omega \approx \omega_c^{(2)} \equiv (g\mu_2)^{1/2}$ and $\omega \approx \omega_0 \equiv g/c_2$ (figure 8). To our knowledge, these features have not previously been studied or identified.

A very strong, by a factor $O(m^{-1})$, amplification of the power flux into the gas occurs in and around the narrow interval of frequencies $\omega_c^{(2)} < \omega < \omega_c^{(3)}$ between the cutoff frequencies $\omega_c^{(2)}$ in (4.11) and $\omega_c^{(3)}$ in (4.16) of the modified surface gravity wave. As shown in § 4.2, this surface wave exists at $\omega < \omega_c^{(2)}$ and $\omega > \omega_c^{(3)}$. The field of the modified surface gravity wave undergoes a qualitative transformation when the frequency increases from $\omega < \omega_c^{(2)}$ to $\omega > \omega_c^{(3)}$: in the gas half-space, the particle displacement exponentially increases with height at the lower frequencies and exponentially decreases with height at the higher frequencies. The bandwidth of

the 'resonance' in the AGW transmission is $\omega_c^{(2)} O(m)$. For the air–water interface, the amplification occurs around 4.0 mHz frequency (wave period of 250 s) and the maximum value of the power flux into air exceeds $22 J_T^{(0)}$ for a source at a depth of $|z_0| = 500$ m (figures 4 and 5). Aside from the relatively small contribution of the modified Lamb wave ($\sim 0.3 J_T^{(0)}$ for the air–water interface when $|z_0| \leqslant 500$ m), the power flux into gas at $\omega_c^{(2)} < \omega < \omega_c^{(3)}$ is due to the body waves, while at $\omega < \omega_c^{(2)}$ and $\omega > \omega_c^{(3)}$ the modified gravity wave makes an appreciable contribution (figure 5).

The sharp increase in amplitude and power flux in the refracted body waves in the gas can be viewed as a direct consequence of the proximity of the two cutoff frequencies of a surface wave. As shown in § 4.2, in the complex q plane (or, more precisely, on the Riemann surface (Brekhovskikh & Godin 1999)), the denominator of the plane-wave transmission coefficient W in (3.7) has two distinct roots, which are defined by $q = \omega^2/g$ and (4.12). The roots are located on the physical sheet ($\operatorname{Im} s_2 > 0$) of the Riemann surface when $\omega < \omega_c^{(2)}$ and $\omega > \omega_c^{(3)}$, respectively. The roots are poles of the integrand in the integral representation (4.3) and (4.4) of the field due to a point source. When located on the physical sheet, the roots correspond to a surface wave. When $\omega_c^{(2)} < \omega < \omega_c^{(3)}$, the poles are on the unphysical sheet ($\operatorname{Im} s_2 < 0$) of the Riemann surface. As long as $m \ll 1$, the poles are close to each other, to the branch cut $\operatorname{Im} s_2(q) = 0$ that connects the physical and unphysical sheets, and to the real q axis. This translates into exceptionally large values of $|W|$ and amplitudes of the refracted plane waves with positive but small values of s_2.

Similar quasi-resonance phenomena are expected to take place in open waveguides and other wave propagation problems where the cutoff frequencies of two normal modes approach each other.

As at $\omega \approx \omega_c^{(2)}$, we again encounter a close approach of two poles, but of a more familiar kind, when $\omega \approx \omega_0 \equiv g/c_2$. The resonance-like amplification of the AGW transmission at $\omega \approx \omega_0$ does not involve a continuous spectrum of the problem (i.e. body waves) (figure 8). The dispersion curves of the Lamb and surface gravity waves, which exist in the limit $m \to 0$, i.e. in a gas half-space with a rigid boundary and in a liquid half-space with a free surface, intersect at $\omega = \omega_0$. For small but finite values of the density ratio m, the dispersion curves of the modified Lamb and surface gravity waves split and recombine (figure 3), with the difference between the phase speeds of the resulting fast and slow surface waves being $c_2 O(m^{1/2})$ at $\omega \approx \omega_0$. The amplitudes of the two surface waves also become very close at $\omega \approx \omega_0$. This leads to a strong interference of the surface waves and deep oscillations with range in the power fluxes carried by the surface waves in the gas and liquid (figure 7*a,b*). At $\omega \approx \omega_0$, a source radiates nearly the same amount of energy into the fast and slow surface waves, and the power fluxes carried by each surface wave are almost equally partitioned between the gas and the liquid half-spaces. In a narrow frequency band of width $\omega_0 O(m^{-1/2})$ around ω_0, the maximum power transmitted into the gas is amplified by a factor $O(m^{-1})$ compared to its value at frequencies away from ω_0. In particular, for the air–water interface, the maximum transmitted power exceeds $26 J_T^{(0)}$ for a source at a depth of $|z_0| = 500$ m (figures 7*a* and 8*b*).

7. Conclusion

Acoustic-gravity waves generated by sources within a liquid can be efficiently transmitted into a gas despite the large contrast in mass density and, possibly, sound speed across the gas–liquid interface. In addition to the refraction of body waves at the interface, the generation of surface waves plays a crucial role in the AGW

transmission. For air–water interfaces, the transmitted power can exceed the total power emitted by the same point source in unbounded water by an order of magnitude or more, depending on wave frequency. The simultaneous account of gravity and fluid compressibility leads to a richer and more complex wave physics and suggests additional mechanisms of atmospheric manifestations of underwater perturbations.

The ratio of gas and liquid densities at the interface is the small parameter that enables a systematic asymptotic analysis of the AGW transmission problem. The results reported here refer to a highly idealized environmental model, where a plane interface separates gas and liquid half-spaces with different but constant sound speeds and buoyancy frequencies. While the physical effects considered in this paper are expected to control the AGW transmission through the air–sea interface, further research is necessary to take into account finite ocean depth, generic density and sound-speed stratifications, wind and other properties of the real ocean and atmosphere.

Acknowledgements

Stimulating discussions with B. Cornuelle, V. V. Goncharov, C. W. Holland, L. A. Ostrovsky and A. G. Voronovich and helpful suggestions of three anonymous referees are gratefully acknowledged. This research has been supported in part by the U.S. Navy under STTR contract N06-T002.

REFERENCES

ABRAMOWITZ, M. & STEGUN, I. A. (Eds) 1965 *Handbook of Mathematical Functions with Formulas, Graphs, and Mathematical Tables*. Dover.

ADAM, J. A. 1977 Solutions of the inhomogeneous acoustic-gravity wave equation. *J. Phys.* A: *Math. Gen.* **10**, L169–L173.

ARTRU, J., DUCIC, V., KANAMORI, H., LOGNONNÉ, P. & MURAKAMI, M. 2005 Ionospheric detection of gravity waves induced by tsunamis. *Geophys. J. Intl* **160**, 840–848.

BREKHOVSKIKH, L. M. & GODIN, O. A. 1998 *Acoustics of Layered Media 1: Plane and Quasi-Plane Waves*, 2nd edn. Springer.

BREKHOVSKIKH, L. M. & GODIN, O. A. 1999 *Acoustics of Layered Media 2: Point Sources and Bounded Beams*, 2nd edn. Springer.

BREKHOVSKIKH, L. M. & GONCHAROV, V. 1994 *Mechanics of Continua and Wave Dynamics*, 2nd edn., chap. 10. Springer.

DROB, D. P., GARCÉS, M., HEDLIN, M. & BRACHET, N. 2010 The temporal morphology of infrasound propagation. *Pure Appl. Geophys.* **167**, 437–453.

ECKART, C. 1960 *Hydrodynamics of Oceans and Atmospheres*. Pergamon.

EVERS, L. G. & HAAK, H. W. 2001 Listening to sounds from an exploding meteor and oceanic waves. *Geophys. Res. Lett.* **28**, 41–44.

FUKS, I. & GODIN, O. A. 2011 Generation of acoustic-gravity waves by a submerged monopole source located near the water–air interface. In *OCEANS'11, MTS/IEEE Conference Proceedings, IEEE, Kona, Hawaii, 19–22 September*, pp. 1–10. Marine Technology Society.

GASILOVA, L. A, GORDEEVA, I. YU. & PETUKHOV, YU. V. 1992 Generation of a modified Lamb surface wave in the atmosphere by an underwater source. *Sov. Phys. Acoust.* **38**, 567–570.

GASILOVA, L. A., GORDEEVA, I. YU. & PETUKHOV, YU. V. 1993 Generation of a Stoneley–Scholte–Lamb atmospheric surface-wave by an acoustic source located in an ocean wave-guide. *Acoust. Phys.* **39**, 19–23.

GASILOVA, L. A. & PETUKHOV, YU. V. 1993 Influence of gravity-waves in the ocean on atmospheric surface-wave excitation by an underwater source. *Acoust. Phys.* **39**, 428–434.

GASILOVA, L. A. & PETUKHOV, YU. V. 1999 Theory of surface waves propagating along sharp boundaries in the atmosphere. *Izv. Akad. Nauk. Fiz. Atm. Okeana* **35**, 14–23.

GODIN, O. A. 1997 Reciprocity and energy theorems for waves in a compressible inhomogeneous moving fluid. *Wave Motion* **25**, 143–167.

GODIN, O. A. 2004 Air–sea interaction and feasibility of tsunami detection in the open ocean. *J. Geophys. Res.* **109**, C05002.

GODIN, O. A. 2006*a* Calculation of amplitudes of acoustic normal modes from the reciprocity principle. *J. Acoust. Soc. Am.* **119**, 2096–2100.

GODIN, O. A. 2006*b* Anomalous transparency of water–air interface for low-frequency sound. *Phys. Rev. Lett.* **97**, 164301.

GODIN, O. A. 2007 Transmission of low-frequency sound through the water-to-air interface. *Acoust. Phys.* **53**, 305–312.

GODIN, O. A. 2008*a* Low-frequency sound transmission through a gas–liquid interface. *J. Acoust. Soc. Am.* **123**, 1862–1879.

GODIN, O. A. 2008*b* Sound transmission through water–air interfaces: new insights into an old problem. *Contemp. Phys.* **49**, 105–123.

GODIN, O. A., IRISOV, V. G., LEBEN, R. R., HAMLINGTON, B. D. & WICK, G. A. 2009 Variations in sea surface roughness induced by the 2004 Sumatra–Andaman tsunami. *Nat. Hazards Earth Syst. Sci.* **9**, 1135–1147.

GODIN, O. A. 2011 Low-frequency sound transmission through a gas–solid interface. *J. Acoust. Soc. Am.* **129**, EL45–EL51.

GODIN, O. A. 2012*a* Incompressible wave motion of compressible fluids. *Phys. Rev. Lett.* **108**, 194501.

GODIN, O. A. 2012*b* Acoustic-gravity waves in atmospheric and oceanic waveguides. *J. Acoust. Soc. Am.* **132**, 657–669.

GOSSARD, E. & HOOKE, W. 1975 *Waves in the Atmosphere*. Elsevier.

HRISTOV, T. S., MILLER, S. D. & FRIEHE, C. A. 2003 Dynamical coupling of wind and ocean waves through wave-induced air flow. *Nature* **422**, 55–58.

LAMB, H. 1911 On atmospheric oscillations. *Proc. R. Soc. Lond.* A **84**, 551–572.

LAMB, H. 1932 *Hydrodynamics*, 6th edn. Cambridge University Press.

LIGHTHILL, J. 1978 *Waves in Fluids*. Cambridge University Press.

MCDONALD, B. E. & CALVO, D. C. 2007 Enhanced sound transmission from water to air at low frequencies. *J. Acoust. Soc. Am.* **122**, 3159–3161.

KEMBALL-COOK, S. & WANG, B. 2001 Equatorial waves and air–sea interaction in the boreal summer intraseasonal oscillation. *J. Clim.* **14**, 2923–2942.

PETUKHOV, YU. V. 1992 Generation of a modified Lamb surface wave in the atmosphere by an underwater source. *Sov. Phys. Acoust.* **38**, 407–410.

PIERCE, A. D. 1963 Propagation of acoustic-gravity waves from a small source above the ground in an isothermal atmosphere. *J. Acoust. Soc. Am.* **35**, 1798–1807.

PIERCE, A. D. 1965 Propagation of acoustic-gravity waves in a temperature- and wind-stratified atmosphere. *J. Acoust. Soc. Am.* **37**, 218–227.

PRESS, F. & HARKRIDER, D. G. 1962 Propagation of acoustic-gravity waves in the atmosphere. *J. Geophys. Res.* **67**, 3889–3908.

ROLLAND, L. M., OCCHIPINTI, G., LOGNONNÉ, P. & LOEVENBRUCK, A. 2010 Ionospheric gravity waves detected offshore Hawaii after tsunamis. *Geophys. Res. Lett.* **37**, L17101.

SAVINA, O. N. 1997 Surface waves at a temperature drop in atmosphere. *Izv. Akad. Nauk. Fiz. Atm. Okeana* **33**, 48–52.

SULLIVAN, P. P. & MCWILLIAMS, J. C. 2010 Dynamics of winds and currents coupled to surface waves. *Annu. Rev. Fluid Mech.* **42**, 19–42.

TOLSTOY, I. 1963 The theory of waves in stratified fluids including the effects of gravity and rotation. *Rev. Mod. Phys.* **35**, 207–230.

TOLSTOY, I. 1973 *Wave Propagation*. McGraw-Hill.

THOME, G. 1968 Long-period waves generated in the polar ionosphere during the onset of magnetic storms. *J. Geophys. Res.* **73**, 6319–6336.

WATADA, S. 2009 Radiation of acoustic and gravity waves and propagation of boundary waves in the stratified fluid from a time-varying bottom boundary. *J. Fluid Mech.* **627**, 361–377.